Bull Volcanol (1999) 61:363–381

ORIGINAL PAPER

D. A. Clague · J. T. Hagstrum · D. E. Champion
M. H. Beeson

Kīlauea summit overflows: their ages and distribution in the Puna District, Hawai'i

Received: 10 October 1998 / Accepted: 12 May 1999

Abstract The tube-fed pāhoehoe lava flows covering much of the northeast flank of Kīlauea Volcano are named the 'Ailā'au flows. Their eruption age, based on published and six new radiocarbon dates, is approximately AD 1445. The flows have distinctive paleomagnetic directions with steep inclinations (40°–50°) and easterly declinations (0°–10°E). The lava was transported ~40 km from the vent to the coast in long, large-diameter lava tubes; the longest tube (Kazumura Cave) reaches from near the summit to within several kilometers of the coast near Kaloli Point. The estimated volume of the 'Ailā'au flow field is 5.2±0.8 km^3, and the eruption that formed it probably lasted for approximately 50 years. Summit overflows from Kīlauea may have been nearly continuous between approximately AD 1290 and 1470, during which time a series of shields formed at and around the summit. The 'Ailā'au shield was either the youngest or the next to youngest in this series of shields. Site-mean paleomagnetic directions for lava flows underlying the 'Ailā'au flows form only six groups. These older pāhoehoe flows range in age from 2750 to <18,000 BP, and the region was inundated by lava flows only three times in the past 5000 years. The known intervals between eruptive events average ~1600 years and range from ~1250 years to >2200 years. Lava flows from most of these summit eruptions also reached the coast, but none appears as extensive as the 'Ailā'au flow field. The chemistry of the melts erupted during each of these summit overflow events is remarkably similar, averaging approximately 6.3 wt.% MgO near the coast and 6.8 wt.% MgO near the summit. The present-day caldera probably formed more recently than the eruption that formed the 'Ailā'au flows (estimated termination ca. AD 1470). The earliest explosive eruptions that formed the Keanakāko'i Ash, which is stratigraphically above the 'Ailā'au flows, cannot be older than this age.

Key words Kīlauea Volcano · Summit eruptions · Radiocarbon dates · Paleomagnetism · Lava tubes · Puna District · Hawai'i · USA

Editorial responsibility: D. A. Swanson

David A. Clague (✉)
Monterey Bay Aquarium Research Institute, P.O. Box 628,
7700 Sandholdt Road, Moss Landing, California 95039, USA
e-mail: clague@mbari.org
Fax: +831-7751645

Jonathan T. Hagstrum · Melvin H. Beeson
Duane E. Champion
United States Geological Survey, 345 Middlefield Road,
MS 937, Menlo Park, California 94025, USA

Introduction

Much of the north flank of Kīlauea Volcano, Hawai'i, is covered by young, glassy, tube-fed lava flows erupted from Kīlauea's summit region (Fig. 1). Named after 'Ailā'au, the Hawaiian god of fire who inhabited Kīlauea Iki and then Kīlauea Crater before fleeing upon Pele's arrival (Westervelt 1916), these flows were produced by a long-sustained eruption from a vent near the eastern end of Kīlauea Iki. A separate lobe of 'Ailā'au flows extends southward from Kīlauea Iki to the coast (Fig. 1). Despite a high average rainfall in the Puna District of ~380 cm/year, the 'Ailā'au flows are little weathered and support only juvenile forest, indicating that they are relatively young (Holcomb 1987). Kīlauea's historical volcanic activity, however, has been confined to its rift zones and summit region. The north flank has been extensively developed during the past 50 years (Fig. 1).

Kīlauea is the most active of the Hawaiian volcanoes, and approximately 90% of its surface lava flows are less than 1100 years old (Holcomb 1987). The 'Ailā'au flows are of particular interest in understanding the volcanic behavior and hazards of Kīlauea, because they presently cover the largest subaerial region on the volcano related to a single eruption (see Wolfe and Morris 1996a). Hazard zones for lava flows have

PACIFIC
OCEAN
KEA`AU RANCH
PAHOA NORTH
PAHOA SOUTH
HILO
MOUNTAIN VIEW
KALALUA
PU`U MAKA`ALA
VOLCANO
MAKAOPUHI CRATER
Kalele
Paki Bay
Keauhou
Kaloli Point
`Auwae
`Opihi Rock
Hawaiian Paradise Park
Hawaiian Beaches
Pahoa
Kea`au
Mountain View
Orchid Land Estates
Hawaiian Acres
Ainaloa
Crescent Acres
Eden Rock Estates
Fern Forest Vacation Estates
Hawaiian Orchid Island Estates
Royal Hawaiian Estates
Maunaloa Estates
Volcano
Wung Quarry
Kazumura Cave
Nahuku (Thurston) Lava Tube
Kilauea Iki
19.625°N
19.500°N
205.000°E
204.875°E
0
5
km
`Aila`au
Cape Kumukahi
Kilauea
Hawai`i
Upolu Point
Keahole Point
Ka Lae
20°N
19°N
205°E
204°E
9B145
B3344
B3332
B3380, WW619
B6783
B6775
B2306
8B181
8B109
8B085
8B193
W4661
W4449
3631
8B169
8B073
8B061
9B133, W3941
B3542
B3566
8B805
8B001
8B049
8B217
9B889, W4177
B3554
B3446
9B433, W4573
B3434
B3410
9B673
9B121
WW620
B3422
8B793, W3881
B3392, B3397
9B427
9B421
WW117
W5631
9B397
9B001, W4162
8B421, W3885
3A364
8B733
WW308
8B541
W4337
1B432
AA10602
W5110
`Apua Point
(see northern continuation below)
(see southern continuation above)

Fig. 1 Map of the north flank of Kīlauea Volcano (see *inset map*) showing the ʻAilāʻau lava flows, their kipukas, paleomagnetic (*dots*) and ^{14}C (*triangle* if charcoal sample only) sampling sites, Nāhuku (Thurston) Lava Tube, Kazumura Cave (Allred and Allred 1997), additional known ʻAilāʻau lava tubes, and the outlines of housing developments predominantly within the ʻAilāʻau flows (mapping modified from Holcomb 1987; Moore and Trusdell 1991; Buchanan-Banks 1993; Wolfe and Morris 1996a). A lobe of ʻAilāʻau lava that flowed to the south is shown as an *inset*. Names of the 7.5-min topographic maps are in the lower right or upper left part of each *quadrangle* shown. A detailed sample map is shown in Fig. 2 for the northeastern coastal portion of the region. A legend for the different stipple patterns for kipukas within the ʻAilāʻau flows is given in the inset to Fig. 2

been assigned to Kīlauea's surface based chiefly on coverage patterns of the recent past (Mullineaux et al. 1987; Wright et al. 1992). The most hazardous areas are in vent regions at the summit and along rift zones and are assigned to hazard zone 1, areas adjacent to and downslope of the active rift zones are assigned to zone 2, and the north and southwest flanks are assigned to zone 3. In zone 3, less than 5% of the area has been covered with lava during historical time, although 75% of the area is thought to have been covered within the past 750 years (Mullineaux et al. 1987).

This study of the ʻAilāʻau flows and their kipukas was undertaken to help decipher the timing and extent of lava accumulation on the north flank of Kīlauea Volcano during the last few millennia and to determine the history of the ʻAilāʻau eruption. Ages of flows are inferred from radiocarbon dates, stratigraphy, and paleomagnetic data referenced to a paleosecular variation (PSV) curve for Hawaiʻi (Hagstrum and Champion 1995).

Moreover, we know little about the durations of sustained eruptions at Kīlauea Volcano. Information about the duration of previous sustained Kīlauea eruptions should provide some guidelines on the possible duration of Kīlauea's ongoing eruption, which began in January 1983 and is now in its seventeenth year. The ʻAilāʻau flow field is the most voluminous and perhaps represents the longest-duration eruption from a single vent recorded on Kīlauea's surface, although how long it actually lasted is uncertain. The present-day caldera existed prior to the explosive eruptions that formed the Keanakākoʻi Ash in AD 1790 (Christiansen 1979; McPhie et al. 1990) or perhaps prior to 1790 (Swanson et al. 1998); the ʻAilāʻau flows almost certainly predate formation of the present-day caldera. Thus, the age and duration of the ʻAilāʻau eruption provides important information on the timing of major changes in the magmatic system at Kīlauea. The ages of the ʻAilāʻau flows and their kipukas also provide a direct long-term measure of the frequency of caldera overflows on the north flank of Kīlauea. These issues are addressed in our detailed study of the ʻAilāʻau and earlier summit eruptions that inundated Kīlauea's northern surface and are essential for evaluating long-term eruptive behaviors at the summit and volcanic hazards in the Puna District.

Previous work

The ʻAilāʻau flows were named by Holcomb (1987) and mapped by him based mainly on the interpretation of aerial photographs supplemented by paleomagnetic determinations. It was the distinctive paleomagnetic direction of the ʻAilāʻau flows (inclinations between 40 and 50°, and easterly declinations between 0 and 10°) that allowed Holcomb (1987) to determine the extent of these flows.

Moore and Trusdell (1991) mapped the northeastern part of the region during their study of the lower east rift zone of Kīlauea Volcano. Buchanan-Banks' (1993) Hilo quadrangle map includes the northwestern corner of the ʻAilāʻau flow field. These previous mapping efforts established that the ʻAilāʻau flows cover most of the northeastern portion of Kīlauea Volcano northwest of its east rift zone. Numerous kipukas that occur within the ʻAilāʻau flows were predominantly mapped from vegetation changes and development of drainage systems as seen in aerial photographs (Holcomb 1987). The kipukas were divided into several age groups (Fig. 1), with one including lava flows from Mauna Loa Volcano (Holcomb 1987; Wolfe and Morris 1996a).

Table 1 lists 13 previously published radiocarbon ages for charcoal collected beneath what have been mapped as ʻAilāʻau flows. A single date reported by Rubin et al. (1987; W4337; Table 1) was not included in Holcomb's (1987) analysis, because it was thought to date a different flow. However, more recent mapping (Neal and Lockwood, in press) places this sample beneath the ʻAilāʻau flows. These published ages (Fig. 1; Table 1) range from 2160 to <200 radiocarbon years BP (Holcomb 1987; Rubin et al. 1987; Wolfe and Morris 1996b; Neal and Lockwood, in press). Holcomb (1987) regarded three of these ages (2160, <200, <200 radiocarbon years BP) as unreliable, because they were superceded by other samples from the same sites. We concur with his assessment of these ages. Holcomb (1987) averaged the remaining four ^{14}C dates to calculate a mean ^{14}C age of 335 BP (between ca. AD 1525 and 1630 calendar years), but assigned the ʻAilāʻau flows to the next older time bracket (350–500 calendar years BP, or AD 1450–1600) on his map. Holcomb et al. (1986) used some additional stratigraphic constraints to estimate an average age of approximately 400 calendar years BP, or AD 1550 for the flow field.

Although eruptions of several types occur within the summit region of Kīlauea Volcano, those of longer duration are more characteristic (Holcomb 1987). Such long-sustained eruptions produce large lava shields and pāhoehoe lava flows that show increased channelization with time, leading to the formation of lava tubes (Swanson 1973; Peterson and Swanson 1974; Peterson et al. 1994). The ʻAilāʻau lava shield is partially preserved around its source vent at the eastern end of Kīlauea Iki crater, although most of the center of the shield has collapsed. Nāhuku (Thurston) lava tube and

Table 1 ^{14}C ages and calibrated calendar ages for the ‘Ailā‘au flows and their kipukas

Lab ID no. ‘Ailā‘au flows	^{14}C age	Calendar age	λ_s (°)	φ_s (°)	Quadrangle	PM site	Reference
W4573[a]	<200	–	19.576	204.843	Mountain View	9B433	2, 3
W4449	<200	–	19.588	204.983	Mountain View	8B061	2, 3
W5110	230±60	1660	19.317	204.782	Makaopuhi	–	2, 4
W3881	260±70	1650	19.545	204.912	Mountain View	8B793	2, 3
W4162	310±70	1640	19.470	204.830	Volcano	9B001, 8B421	2, 3
W4661	320±70	1530, 1540, 1640	19.553	204.977	Mountain View	–	2, 3
WW117	330±75	1530, 1560, 1630	19.438	204.969	Kalalua	–	4
WW620[a]	350±50	1520, 1590, 1620	19.571	204.929	Mountain View	–	6
AA10602[a]	400±70	1470	19.338	204.776	Makaopuhi	1B432	5
WW308	400±50	1470	19.359	204.765	Makaopuhi	–	5
WW619[a]	420±50	1450	19.586	205.027	Pahoa North	B3380	1
3631[a]	420±50	1450	19.586	204.988	Mountain View	8B169[b]	1
WW371	430±60	1450	19.598	205.065	Pahoa North	B3356	1
W3941	450±60	1440	19.588	204.983	Mountain View	9B133	2, 3
WW1524[a]	520±50	1420	19.583	205.084	PahoaNorth	B6767	1
WW1520[a]	530±50	1420	19.571	205.094	Pahoa North	B6912	1
WW1525	570±40	1415	19.584	205.079	Pahoa North	B6832	1
W5631	580±200	1400	19.508	204.873	Pu‘u Maka‘ala	–	4
W4337	620±70	1320, 1350, 1390	19.336	204.776	Makaopuhi	1B432[b]	2, 4
W3885	2160±70	2140 BP	19.470	204.830	Volcano	9B001, 8B421	2, 3
Kipukas							
AA18815[a]	2604±54	2750 BP	19.593	205.071	Pahoa North	B6735	1
W4177	3690±70	4030 BP	19.582	204.970	Mountain View	9B889	2, 3

Lab ID no. is laboratory identification number of ^{14}C sample (new sample WW371 collected by D. Clague and M. Beeson; samples WW1520, WW1524, WW1525, and 3631 collected by D. Clague; and samples WW619 and AA 18815 collected by D. Clague and G. Clague). ^{14}C age is radiocarbon age in years BP (before present; AD 1950) with uncertainty given as one standard deviation of the counting statistics. Calendar age is calculated using the calibration method of Stuiver and Reimer (1993) and is in years AD unless otherwise indicated. Quadrangle is 7.5-min (1:24,000) USGS topographic map (see Fig. 1). PM site is the corresponding paleomagnetic site in Table 3; λ_s, φ_s north latitude and east longitude of the sampling site. References: *1* this study; *2* Rubin et al. (1987); *3* Holcomb (1987); *4* Wolfe and Morris (1996b); *5* Neal and Lockwood (in press); *6* unpublished data, sample collected by F. Trusdell

[a]Samples that received full pretreatment as explained in the text

[b]Nearby site only

other tubes (Fig. 1) spreading northeastward from the vent area fed the multiple lobes identified at lower (<500 m) elevations (Holcomb 1987). Kazumura Cave, the longest of these lava tubes, extends from near the summit vent almost to the coast ~40 km away (Allred and Allred 1997). All the tubes depicted in Fig. 1 are in the ‘Ailā‘au flows. However, nearly all the kipukas surrounded by the ‘Ailā‘au flows are in pāhoehoe that erupted from near the summit and was presumably transported through lava tubes as well.

Sampling and laboratory methods

Our study of the ‘Ailā‘au flows and their kipukas is based on four types of data: geologic observations and mapping, chemical analyses of glass collected from surfaces of the flows, radiocarbon dating of charcoal collected from beneath the margins of flows, and paleomagnetic data from near-surface drill cores. Our new mapping was restricted mainly to the strip of well-exposed lava flows along the coast (Fig. 2). The purpose of this work was to determine the stratigraphic relations of the different units in the region rather than to improve upon the photogeologic maps published by Holcomb (1987).

The charcoal samples were dried and handpicked to remove modern rootlets. Charcoal samples WW371, WW619, WW620, WW1520, WW1524, and WW1525 were converted to graphite by J. McGeehin at the U.S. Geological Survey's graphite laboratory in Reston, Virginia, and were dated at the Center for Accelerator Mass Spectrometry (AMS) at Lawrence Livermore National Laboratory. Sample 3631 was counted with a gas-flow proportional counter at the U.S. Geological Survey Radiocarbon Laboratory in Menlo Park, California, by D. Trimble. Samples AA10602 and AA18815 were converted to graphite and analyzed by accelerator mass spectrometry by W. Beck at the NSF AMS Facility at the University of Arizona. Ages for both new and previously published ^{14}C determinations are presented in Table 1. The ages were calibrated to calendar years using the Calib 3.0 program of Stuiver and Reimer (1993) and the calibration data from Stuiver et al. (1998). Herein we report the probabilities of different age ranges based on their method B calculations. For completeness, we graphically show the age ranges calculated using their method A.

Dense vegetation on the north flank, particularly in the Volcano and Kalalua quadrangles (Fig. 1), makes access for mapping and sampling purposes exceptionally difficult. Almost all of the glass, charcoal, and paleo-

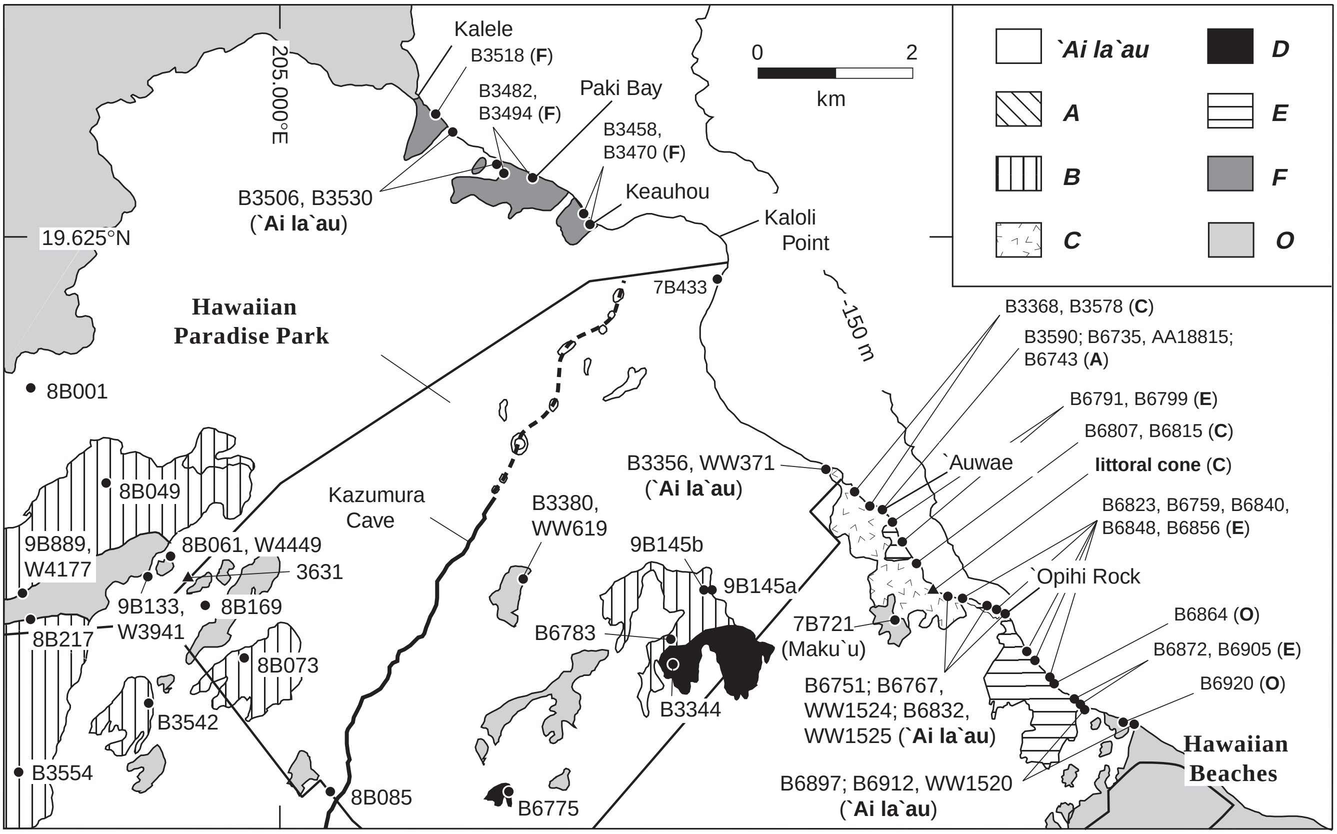

Fig. 2 Map of the coastal section described in the text. Locations of paleomagnetic sites and radiocarbon samples are shown as in Fig. 1. The kipukas, modified from mapping by Holcomb (1987) and Wolfe and Morris (1996a) based on our fieldwork, are grouped into eight flow units (ʻAilāʻau, A, B, C, D, E, F, etc.) based mainly on their paleomagnetic directions. Unit A erupted 2750 BP and unit B 4030 BP. Unit C is inferred to be approximately 5250 BP, unit D is older than 5590 BP and younger than units E and F, and units E and F are probably older than approximately 9000 BP. The "other" unit includes several kipukas with solitary paleomagnetic determinations unlike the labelled units, as well as unsampled kipukas. One of these unsampled kipukas, a sugarcane field south of Keaʻau, is inferred to be a Mauna Loa flow >40,000 BP. The –150 m contour, based on a swath bathymetric Simrad EM300 survey, is along an offshore terrace shown in more detail in Figs. 3 and 4. Elsewhere around the Island of Hawaiʻi, this terrace is a coral reef that drowned at ~18 ka (Ludwig et al. 1991). The Kazumura Cave is shown *dashed* where it is inferred from the locations of shattered rock rings near Kaloli Point. The ʻAilāʻau flow field had only one long-lived ocean entry at Kaloli Point, where lava transported through the Kazamura Cave built a large delta across the flat behind the reef's edge

magnetic samples in this study, therefore, were collected from roadcut or coastal exposures (Fig. 2). Lava flows sampled for chemical analysis were specifically collected because they still had unaltered glassy rinds. Older flows with poor or no glassy rinds were not analyzed. The glass samples were chipped from the flow surface, and multiple chips were mounted and prepared as polished thin sections for electron microprobe analysis. The analyses were performed on a SEMQ microprobe at the U.S. Geological Survey in Menlo Park, California, using natural and synthetic standards. The 74 microprobe analyses have been averaged and normalized to 100% by flow unit and by distance from the vent (Table 2). Four samples having opaque glass and low alkali contents were omitted from Table 2, because we suspect that these samples were altered after quenching and do not represent melt compositions.

Core samples for paleomagnetic analysis were obtained with a portable drill and oriented with a clinometer and both solar and magnetic compasses. Usually 8–12 samples were collected per site (Table 3). The remanent magnetization of individual specimens, cut from the core samples, was measured with either a commercial cryogenic or a spinner magnetometer. After measuring the natural remanent magnetizations, usually two pilot specimens from each site were progressively demagnetized with 400-Hz alternating fields to a maximum field of 100 mT. From these data the optimum level of demagnetization was selected for the remainder of samples from a given site. Generally, these lava flows have very stable remanent magnetizations, and little magnetic cleaning was needed; blanket demagnetization steps were usually ≤30 mT. The statistics of Fisher (1953) were used in analyzing the site- and group-mean directions presented in Table 3.

A bathymetric survey was conducted in February 1998 to determine the extent of the flows offshore. MBARI contracted C&C Technologies to conduct the survey on the M/V Ocean Alert using a hull-mounted 30 kHz multibeam Simrad EM300 system. The survey

Table 2 Normalized microprobe glass analyses for the ‘Ailā‘au flows and their kipukas

Unit	‘Ailā‘au	‘Ailā‘au	‘Ailā‘au	‘Ailā‘au	‘Ailā‘au	‘Ailā‘au	‘Ailā‘au	‘Ailā‘au	A	B	C	F
Number	5	2	10	4	6	2	9	15	1	1	6	9
Distance	0–5	5–10	10–15	15–20	20–25	25–30	30–35	35–40				
Average distance	0.13	6.7	13.0	18.5	22.6	26.6	31.3	38.4	38.6	38.6	38.5	37.5
SiO_2	52.00	51.35	51.81	51.68	51.87	51.57	51.63	51.72	51.21	51.61	51.76	51.55
Al_2O_3	14.01	13.92	14.00	14.00	13.96	13.99	13.76	13.72	13.22	13.84	13.61	13.77
FeO*	10.45	11.07	10.77	10.61	10.77	10.83	11.29	11.36	12.91	11.23	11.71	11.37
MgO	6.87	6.56	6.43	6.78	6.37	6.47	6.35	6.27	5.52	6.88	6.09	6.31
CaO	11.27	11.45	11.24	11.37	11.18	11.29	11.20	11.12	10.29	11.09	10.96	11.15
Na_2O	2.17	2.29	2.32	2.23	2.35	2.37	2.28	2.26	2.54	2.20	2.28	2.27
K_2O	0.39	0.43	0.44	0.43	0.46	0.47	0.44	0.44	0.56	0.37	0.44	0.46
TiO_2	2.46	2.54	2.59	2.52	2.64	2.61	2.64	2.69	3.23	2.41	2.72	2.70
P_2O_5	0.21	0.23	0.24	0.23	0.24	0.23	0.24	0.25	0.33	0.22	0.26	0.26
MnO	0.16	0.17	0.16	0.15	0.16	0.16	0.17	0.17	0.19	0.17	0.17	0.16
S	<0.015	<0.015	<0.015	<0.015	<0.015	<0.015	<0.015	0.007	0.014	0.008	0.010	0.008

Unit indicates stratigraphic unit. *Number* is number of samples within the unit or distance range that have been averaged (each sample analysis itself is an average of six to ten spots). *Distance* for ‘Ailā‘au flows specifies the range of distances from vent (in kilometers) from which samples were collected (location of vent is defined as the center of Kīlauea Iki Crater). *Average Distance* is average of the sample locality distances from vent (in kilometers) for samples in each group

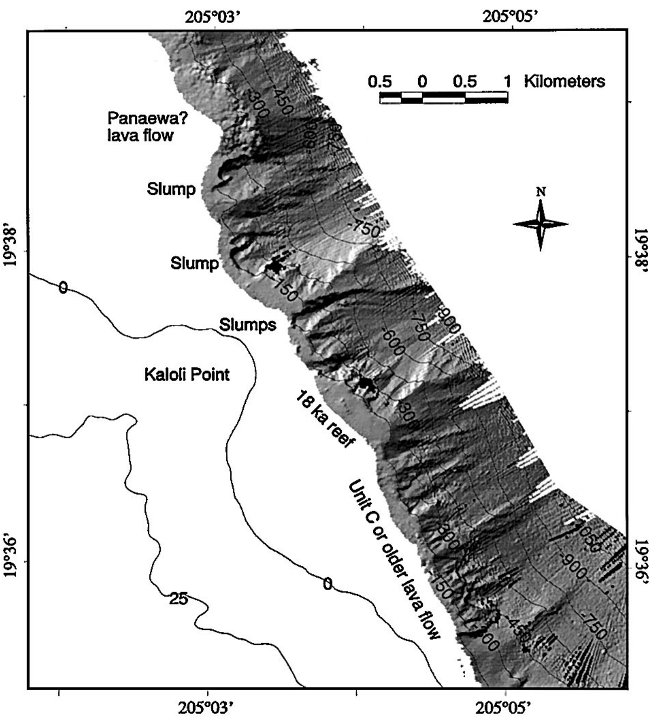

Fig. 3 Bathymetric map of Simrad EM300 swath data. The edge of the 18 ka reef is at approximately –150 m. Shoreward of the reef the bottom is smooth and gently sloping, whereas seaward of the reef edge, the slope increases sharply. Slumps have modified the reef face north and east of Kaloli Point, and two lava flows cross the reef. One lava flow continues north from just north of the northern landslide; it is probably the submarine extension of the 1470 ± 50 radiocarbon years BP Pana‘ewa ‘a‘ā flow from Mauna Loa Volcano (Wolfe and Morris 1996a). It has a hummocky texture, indicative of an ‘a‘ā flow. The southern flow is less rough and has lower relief; it crosses the reef between 19°36.8′N and 19°35.55′N. It is not located offshore of the ‘Ailā‘au flows and, therefore, is probably an older flow, perhaps unit C or an even older flow not exposed on land

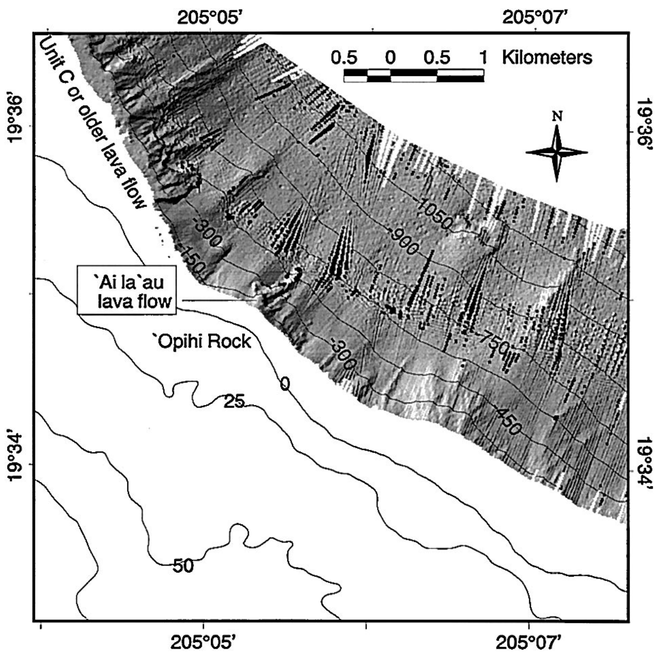

Fig. 4 Bathymetric map of Simrad EM300 swath data, as shown in Fig. 3. The image shows a 0.75-km-long lava lobe extending down the steep flank of the island immediately offshore from ‘Opihi Rock. This lobe is probably of ‘Ailā‘au lava that draped the seacliff and flowed down the offshore slope. This is the only ‘Ailā‘au flow seen in the offshore bathymetry, supporting our contention that almost the entire volume of the ‘Ailā‘au flow field is on land. East of ‘Opihi Rock, the reef is buried beneath younger flows erupted from Kīlauea’s east rift zone. The northwest corner of Fig. 4 overlaps the southeast corner of Fig. 3

lines were navigated using differential GPS and processed on-board. The bathymetric data were gridded at 10 m. The data are presented as sun-illuminated images with the illumination from an azimuth of 315° and an elevation of 45° (Figs. 3, 4).

Table 3 Paleomagnetic data for the ‘Ailā‘au flows and their kipukas

Lab ID no.	λ_s (°)	φ_s (°)	I (°)	D (°)	N/N_0	R	k	α_{95} (°)	λ_p (°)	φ_p (°)
‘Ailā‘au flows (1405–1470 AD)										
8B001[a]	19.608	204.971	43.3	2.0	12/12	11.98430	701	1.6	84.1	222.6
8B061[a]	19.588	204.983	41.2	3.3	12/12	11.98925	1093	1.4	84.9	241.2
8B085[a]	19.562	205.006	42.6	3.7	12/12	11.99259	1484	1.1	83.9	237.8
8B109[a]	19.494	205.038	43.6	5.4	12/12	11.98966	1063	1.3	82.2	244.1
8B169[a]	19.584	204.990	45.3	5.0	12/12	11.99154	1300	1.2	81.5	236.6
8B181[a]	19.513	205.037	43.9	0.4	12/12	11.96629	326	2.4	83.8	208.0
8B193[a]	19.549	205.020	45.2	5.2	12/12	11.99390	1804	1.0	81.4	237.7
8B421[a]	19.470	204.830	44.0	1.5	12/12	11.92823	153	3.5	83.6	216.9
8B541[a]	19.341	204.777	41.9	0.7	11/12	10.99266	1363	1.2	85.2	212.8
8B733[a]	19.42	204.76	43.4	6.3	11/12	10.99128	1147	1.4	81.8	248.3
8B793[a]	19.545	204.912	41.3	5.5	12/12	11.98254	630	1.7	83.4	254.6
9B001[a]	19.470	204.830	43.1	2.7	11/12	10.99267	1365	1.2	83.8	228.5
9B121[a]	19.580	204.938	44.2	3.2	12/12	11.98786	906	1.4	83.0	229.2
9B133[a]	19.588	204.983	45.6	4.2	11/12	10.98108	528	2.0	81.6	231.3
9B145a[a]	19.585	205.051	43.4	8.4	6/6	5.99639	1384	1.8	80.3	257.2
9B397[a]	19.441	204.867	44.7	7.1	12/12	11.90423	115	4.1	80.5	246.9
9B421[a]	19.466	204.906	43.6	5.2	6/6	5.99921	6351	0.8	82.3	242.5
9B427[a]	19.471	204.916	42.0	5.1	4/6	3.99388	490	4.2	83.3	249.0
9B433[a]	19.572	204.941	46.0	3.1	12/12	11.97369	418	2.1	81.7	224.1
9B673[a]	19.492	204.955	39.8	1.6	12/12	11.98476	722	1.6	86.5	230.2
1B432	19.340	204.777	41.2	2.2	9/12	8.97464	316	2.9	85.2	229.7
3A364	19.453	204.793	42.6	4.2	13/13	12.98702	925	1.4	83.5	240.8
7B433	19.621	205.051	45.9	6.7	12/12	11.97597	458	2.0	80.2	242.4
B3332[b]	19.545	205.094	49.0	3.3	12/12	11.97919	529	1.9	79.3	220.7
B3356	19.598	205.065	44.3	2.6	12/12	11.99023	1126	1.3	83.1	225.2
B3380a	19.586	205.027	46.1	3.1	8/8	7.99780	3176	1.0	81.6	224.4
B3392	19.498	204.926	44.2	5.7	9/9	8.99714	2800	1.0	81.7	243.1
B3397	19.498	204.926	46.2	5.3	9/9	8.99687	2552	1.0	80.6	235.1
B3410	19.514	204.951	43.9	4.2	12/12	11.99243	1453	1.1	82.7	236.3
B3422	19.534	205.933	45.5	3.7	12/12	11.99353	1700	1.1	81.8	228.8
B3506	19.633	205.026	47.9	4.9	12/12	11.98825	936	1.4	79.6	229.7
B3530	19.637	205.020	46.1	3.8	11/12	10.99599	2494	0.9	81.4	228.1
B6751	19.582	205.085	46.8	8.9	8/8	7.99520	1458	1.5	78.3	247.2
B6767	19.583	205.084	46.0	5.1	8/8	7.98962	674	2.1	80.9	235.0
B6832	19.584	205.079	45.3	6.2	8/8	7.98049	359	2.9	80.9	242.2
B6897	19.569	205.101	50.6	3.1	8/8	7.96417	195	4.0	78.0	217.7
B6912	19.571	205.094	48.3	1.6	5/8	4.99746	1572	1.9	80.1	213.3
Average	19.532	204.966	44.6	4.2	37/37	36.96002	900	0.8	82.3	234.0
Kipukas										
A (~2750 BP)										
8B805[a]	19.510	204.990	21.2	354.7	12/12	11.99055	1163	1.3	80.0	56.7
B3590	19.594	205.070	18.2	356.1	12/12	11.98060	567	1.8	79.1	45.6
B6735	19.593	205.071	19.5	358.8	7/8	6.98605	430	2.9	80.4	32.0
B6743	19.593	205.072	17.5	357.1	8/8	7.99661	2068	1.2	79.0	40.2
Average	19.573	205.051	19.1	356.7	4/4	3.99759	1242	2.6	79.7	43.7
B (~4030 BP)										
8B049[a]	19.597	204.980	33.1	0.8	12/12	11.98680	833	1.5	88.3	0.2
8B073[a]	19.577	204.995	35.1	0.5	12/12	11.99463	2047	1.0	89.5	316.8
8B217[a]	19.582	204.971	36.4	4.0	10/12	9.99419	1550	1.2	86.2	284.5
9B145b[a]	19.585	205.051	36.2	7.5	6/6	5.99418	859	2.3	82.9	289.9
9B889[a]	19.584	204.969	36.1	0.1	12/12	11.99065	1177	1.3	89.5	218.5
B3434	19.562	204.952	34.6	3.0	12/12	11.99422	1903	1.0	87.1	304.9
B3446	19.541	204.964	37.2	6.2	12/12	11.99001	1101	1.3	84.1	282.0
B3542	19.571	204.983	36.0	7.1	12/12	11.98651	815	1.5	83.3	290.5
B3554	19.564	204.969	36.6	3.7	12/12	11.99598	2733	0.8	86.4	281.6
B3566	19.549	204.992	32.8	1.5	11/12	10.98866	882	1.5	88.3	8.9
B6783	19.579	205.046	35.1	5.1	8/8	7.99083	763	2.0	85.2	296.6
Average	19.572	204.988	35.4	3.6	11/11	10.98977	977	1.5	86.6	294.5
C (~5400–5100 BP)										
B3368	19.595	205.068	44.1	1.0	12/12	11.99411	1866	1.0	83.7	213.6
B3578	19.594	205.070	41.6	2.6	12/12	11.99114	1241	1.2	85.0	233.4
B6807	19.588	205.075	42.8	0.3	8/8	7.99115	791	2.0	84.7	208.0
B6815	19.588	205.075	43.1	3.1	8/8	7.99431	1231	1.6	83.8	231.9
Average	19.591	205.072	42.9	1.8	4/4	3.99909	3296	1.6	84.4	221.7

Table 3 Continued

Lab ID no.	λ_s (°)	φ_s (°)	I (°)	D (°)	N/N_0	R	k	α_{95} (°)	λ_p (°)	φ_p (°)
D (>5400 and <9000 BP)										
B2306[b]	19.529	205.027	26.4	354.7	12/12	11.99113	1241	1.2	82.4	67.9
B3344	19.576	205.047	25.3	353.6	12/12	11.99321	1620	1.1	81.2	70.3
B6775	19.561	205.028	24.5	350.7	8/8	7.99064	748	2.0	78.8	79.3
Average	19.555	205.034	25.4	353.0	3/3	2.99866	1492	3.2	80.9	73.4
E (~15,000–9000 BP)										
B6759	19.582	205.085	21.8	1.8	8/8	7.99302	1003	1.8	81.6	13.0
B6791	19.592	205.072	21.6	2.9	7/8	6.99473	1140	1.8	81.2	6.4
B6799	19.590	205.073	22.3	3.2	8/8	7.99360	1094	1.7	81.4	3.9
B6823	19.584	205.080	21.1	359.1	9/9	8.98478	526	2.3	81.3	31.1
B6840	19.577	205.088	24.5	1.3	8/8	7.99237	918	1.8	83.2	14.8
B6848	19.577	205.089	22.7	0.1	8/8	7.99321	1031	1.7	82.2	24.7
B6856	19.574	205.091	22.0	4.1	8/8	7.99766	2991	1.0	81.0	358.9
B6872	19.572	205.094	20.0	1.7	7/8	6.99602	1506	1.6	80.6	14.7
B6905	19.571	205.094	20.2	0.5	6/7	5.98757	402	3.3	80.9	22.2
Average	19.580	205.085	21.8	1.6	9/9	8.99509	1628	1.3	81.6	14.1
F (~15,000 to 9000 BP)										
B3458	19.626	205.037	13.7	359.2	11/12	10.98490	662	1.8	77.3	28.6
B3470	19.627	205.036	14.0	359.9	11/12	10.99235	1308	1.3	77.5	25.5
B3482	19.632	205.030	13.1	358.5	11/12	10.97663	428	2.2	76.9	31.6
B3494	19.633	205.026	13.1	359.0	12/12	11.99380	1775	1.0	77.0	29.5
B3518	19.639	205.018	12.3	359.1	11/12	10.98161	544	2.0	76.6	28.7
Average	19.631	205.029	13.2	359.1	5/5	4.99959	9846	0.8	77.1	28.9
Other Kīlauea flows										
7B721	19.581	205.073	22.4	8.9	8/8	7.99043	731	2.7	78.3	336.6
B3380b	19.586	205.027	29.8	2.9	4/4	3.99681	939	3.0	85.4	347.1
B6864	19.574	205.091	33.2	2.4	8/8	7.98953	669	2.1	87.3	328.0
B6920	19.569	205.101	28.1	355.7	8/8	7.92707	96	5.7	83.8	67.7

Lab ID no. is laboratory identification number of paleomagnetic sampling site; λ_s, φ_s north latitude and east longitude of site; *I, D* in situ inclination and declination of mean paleomagnetic directions; N/N_0 no. of samples averaged/no. of samples collected; *R* vector sum of *N* unit vectors; *k* concentration parameter (Fisher 1953); α_{95} radius of 95% confidence; λ_p, φ_p north latitude and east longitude of corrected virtual geomagnetic pole. Ages are in calendar years before present (BP, AD 1950)

[a] Originally published in Holcomb (1981), Holcomb et al. (1986), and Holcomb (1987)

[b] Published in Hagstrum and Champion (1994)

Geologic observations

We incorporate field observations with compositions of surface glass from the flows, radiocarbon dates, and paleomagnetic data to identify specific flow units. The paleomagnetic data, in particular, proved essential to identification of the different flow units. The units are identified as the ʻAilāʻau flows and as six older units, A–F, generally in sequence from youngest to oldest. The details of the paleomagnetic, radiocarbon dating, and glass compositional data are discussed in more detail later. Where appropriate, we indicate the pertinent paleomagnetic sites from Table 3 and radiocarbon sites from Table 1. The detailed sample locations and relationships outlined below are depicted in Fig. 2.

The most striking observation is that the ʻAilāʻau flows did not enter the ocean over nearly as wide an area as previously thought. Moving southeast from Kalele (Fig. 2), the first 0.5 km of coast consists of an old flow (unit F) with almost no surface glass and no sea cliff developed (B3518; Table 3). There is also an extensive boulder bed located roughly 20 m inland. Over the next 0.8 km of coast, mostly young glassy ʻAilāʻau flows are found (B3530 on the northwest and B3506 on the southeast edges, respectively; Fig. 2; Table 3), including one area where these flows overlie and have welded a black sand beach deposit. The sand is fresh and compositionally similar to glass from the tops of ʻAilāʻau flows. It probably formed by steam explosions that produced small, perhaps ephemeral, littoral cones as the ʻAilāʻau flows entered the ocean in a manner analogous to that documented for the on-going Kīlauea eruption (Mattox and Mangan 1997). The ʻAilāʻau flows are only a few meters thick in this area, and small kipukas of the underlying unit F flows are common. The next 1.4 km to Keauhou consists of unit F flows (B3494, B3482, B3470, and B3458; Fig. 2; Table 3). There are basalt cobble beaches (e.g., northwest of Pākī Bay) and basalt and coral sand beaches like those at Pākī Bay. Several narrow lobes of ʻAilāʻau flows overlie unit F and reach the sea, but the widest entry is <20 m wide. They cover and cement cobble beach deposits, and tree molds are common. The surfaces on unit F flows have been broken up extensively and blocks removed by wave action. These blocks form a strandline, and individual blocks are found as far as

150 m inland. Freshwater springs are common along the coast throughout the unit F flows, and the area was populated by Hawaiians, who left numerous petroglyphs and bait-grinding bowls (Kirch 1985) in the flow surfaces.

From Keauhou southeast around Kaloli Point to site B3356 in the Hawaiian Paradise Park subdivision (Fig. 1), the land surface consists only of dense, glassy ‘Ailā‘au flows (7B433 and B3356; Fig. 2; Table 3). Kaloli Point is directly seaward of the Kazumura lava tube, which is mapped to within 6 km of the shoreline (Fig. 2). Its continuation to Kaloli Point can be inferred from a series of shattered rock rings (Kauahikaua et al. 1998) above the tube. The ‘Ailā‘au flows entered the ocean across a zone approximately 4 km wide, and the Kaloli Point lava delta has extended the original shoreline approximately 1.1 km seaward. Almost this entire section of coast has sea cliffs averaging approximately 5–6 m high. Only rare lava blocks or boulders carried inland by storms or tsunamis rest on the ‘Ailā‘au flows, and wave action has done little to modify the original lava surface. The southeasternmost kilometer of sea cliffs consists of ‘Ailā‘au flows overlying an older unit (unit C?) that is exposed only in the cliff. The sea cliff around Kaloli Point consists only of ‘Ailā‘au flows. No evidence of Hawaiian activity or petroglyphs was locally observed on the ‘Ailā‘au flows.

At site B3356 (Fig. 2, Table 3), ‘Ailā‘au flows (WW371, Table 1) overlie unit C flows exposed in numerous kipukas. Molds of coconut and pandanus trees are common in the overlying ‘Ailā‘au flows along the coastal cliffs. The point of land 0.6 km northwest of ‘Auwae Point is formed by a large tumulus that may represent the coastal termination of a major lava tube in unit C flows. Coarse-grained soils altered from littoral black sand deposits are interbedded with lava in the tumulus, indicating proximity to littoral explosions where lava entered the ocean. ‘Ailā‘au flows cover a cobble-and-boulder beach, cementing many of the boulders together. Tree molds also are common in the ‘Ailā‘au flows. The most southeasterly ‘Ailā‘au flow in this area drapes a unit C flow another hundred meters farther southeast. The next 0.4 km of coast to the southeast consists of unit C flows (B3368 and B3578; Fig. 2; Table 3), which form a low sea cliff averaging approximately 2–2.5 m high. The relatively flat top of the sea cliff has been heavily modified by wave action. Blocks up to 2 m across have been ripped up and deposited in a strandline, as seen inland on the unit F flows, but are absent on ‘Ailā‘au flows. Individual blocks are found as far as 100 m inland of the strandline. Unlike on unit F, no sand beaches occur on the unit C flows. The exposed lava surface here is the interior lower surface of flat, wide, gas pockets of inflated flows. The tops have been removed by wave action. Unit C flows also have Hawaiian bait bowls (Kirch 1985) carved in the rock near the waterline.

Approximately 100 m northwest of ‘Auwae Point (Fig. 2), unit C flows are covered by unit A flows that form the point. The unit A flows are only 0.2–0.3 km wide (see Fig. 2; B3590, B6735, and B6743; Table 3). A charcoal sample (AA18815; Table 1) was collected from a fine-grained soil layer 2–3 cm thick under the northwestern edge of this flow where it laps onto unit C flows. ‘Auwae Point itself is a thick inflated flow with abundant vertical tree molds in its upper surface and several 1.5-m diameter inflation pits that are several meters deep. The sea cliff of unit A flows averages approximately 3–3.5 m high, and the upper surface has not been broken up by waves. Boulders from nearby unit C flows, however, are strewn inland for at least 50 m. Unit A flows are covered by a thin (<1 m) carbonate shelf just southeast of ‘Auwae Point. This carbonate, formed by chemical precipitation above freshwater springs, cements basalt cobbles and pebbles within a hardpan.

The ‘Auwae Point unit A pāhoehoe flows overlie unit E pāhoehoe flows to the southeast. Unit E is less than 0.1 km wide (see Fig. 2; B6791 and B6799, Table 3), has no sea cliff, and has an upper surface that is no longer glassy. Hawaiian petroglyphs, bait bowls, and kōnane board games (Kirch 1985) are carved in its upper surface, including some now located below the high-tide waterline. Hawaiians almost certainly did not carve these below the high tide line. Instead, the flows have slowly subsided with the rest of the island at approximately 2.5 mm/year (Moore and Fornari 1984). An extensive boulder strandline occurs approximately 15 m inland from the coast. Farther southeast, another 0.7-km-wide section of unit C flows overlies the unit E flows. These flows closely resemble the other unit C flows to the northwest in terms of cliff height and boulder strandline. Inland from this area, a large Hawaiian village site named Maku‘u was located on a picrite flow with a distinct paleomagnetic direction (7B721, Table 3). A direction with similar inclination but more easterly declination distinguishes the Maku‘u site from unit E flows.

Toward the southeastern end of this unit C exposure, the old sea cliff retreats ~ 20 m inland from the present coastline. A younger flow spread along the base of the cliff and inflated to form an elongate tumulus parallel to the coast. It is similar to those formed during the current eruption of Kīlauea at the base of a sea cliff as the lava spreads along the coast to form a narrow bench or shelf. The flow seaward of the cliff here is also likely to be unit C lava, emplaced after the cliff developed. The unit C flows that form the cliff and those that form the elongate tumuli at the base of the cliff probably formed within weeks of each other. Along Kīlauea’s south coast, sea cliffs commonly develop during flow emplacement as a result of slumping. The entire section exposed in this paleo-sea cliff consists of unit C flows (B6807 at top and B6815 at base; Fig. 2; Table 3). The cliff increases in height to ~ 15–20 m toward the southeast around a small embayment, and these flows overlie a truncated littoral cone that consists mainly of cinder. Immediately southeast of the littoral cone a sea cliff of similar height continues for ~0.3 km. This section was not accessible to us but probably consists of unit C flows; thus, the total width of unit C flows southeast of ‘Auwae Point, including the littoral cone, is approximately 1.4 km.

Starting ~0.7 km northwest of ‘Opihi Rock (Fig. 2), the sea cliff decreases to approximately 6 m in height, and a flat surface occurs inland of the sea cliff. The flows at this location consist almost entirely of unit E flows (B6823 and B6759; Table 3). Several narrow (10–30 m wide), thin (<1–3 m thick) ‘Ailā‘au flows (B6751, B6832, and B6767; Table 3) occur atop these unit E flows. These ‘Ailā‘au flows are dense and glassy, have elongate vesicles, and are identical in appearance to ‘Ailā‘au flows found further northwest near Kaloli Point. Several of these ‘Ailā‘au flows reach the sea cliff (e.g., one at ‘Opihi Rock; B6751; Table 3), and several others end within 20 m of the sea cliff (B6767; Table 3). Two charcoal samples (WW1524 and WW1525; Table 1) were collected below these flows in a soil layer that varies in thickness but averages 10–15 cm thick. The soil consists of fine-grained altered ash redistributed by wind and water into drifts nearly 50 cm thick prior to arrival of the overlying ‘Ailā‘au flows. Morphologically variable unit E flows occur southeast of ‘Opihi Rock for approximately 1.6 km (B6840, B6848, B6856, B6872, and B6905; Fig. 2; Table 3) with only two narrow lobes of ‘Ailā‘au flows reaching the sea cliff (B6912; Table 3). These unit E flows have no glass remaining on their upper or lower surfaces and lack the strandline of boulders that occurs along other old sections of coast to the northwest. The higher sea cliff here presumably has prevented deposition of boulders atop these flows.

Two ‘a‘ā lava flows crop out along the coast approximately 1.1 km (B6864; Table 3) and 0.5 km (B6920; Table 3) northwest of the Hawaiian Beaches subdivision (Fig. 2). The southeastern ‘a‘ā flow is on top of unit E flows. It also has the same paleomagnetic direction as site 9B853 on Pāpio Street in Hawaiian Beaches that was assigned an age of ~1300 radiocarbon years old by Hagstrum and Champion (1994). It is separated from the main portion of the flow in Hawaiian Beaches by a lobe of ‘Ailā‘au lava (B6897, Table 3; WW1525, Table 1). The northwestern ‘a‘ā appears to underlie unit E flows based on topography, although the contacts are not well exposed, and has a paleomagnetic direction not seen elsewhere in the area.

Several additional sites provide important information in deciphering the stratigraphy and history of the area. Near the center of the Hawaiian Paradise Park subdivision, an ‘Ailā‘au flow and a lower flow beneath a thin intervening soil layer (2–3 cm thick) were both sampled at site B3380 (Fig. 2; Table 3). The lower flow has a paleomagnetic direction different from that of any flows sampled nearby. A charcoal sample (WW619; Table 1) was collected from the soil beneath the ‘Ailā‘au flow at this site. At another site in Paradise Park, an ‘Ailā‘au flow and an underlying unit B flow were both sampled (site 9B145; Fig. 2; Table 3); these flows crop out on opposite sides of Maku‘u Drive, and the contact is now paved over. At paleomagnetic site B6775, a unit D flow is covered by an irregular soil averaging ~10 cm in thickness.

Offshore geology

The bathymetric survey conducted offshore provides information on several aspects of the local geology. The development of sea cliffs appears to be directly related to the offshore bathymetry and geology. Northwest of the littoral cone just northwest of ‘Opihi Rock, a drowned reef is found offshore, at approximately –150 m depth, that continues around the entire northern and western coasts of Hawai‘i as far south as Kealakekua Bay. Corals collected from the reef's break-in-slope at several sites around the island have been dated using $^{234}U/^{238}U$ at approximately 18,000 years B.P. (Ludwig et al. 1991). The reef formed at sea level and has become submerged due to the combined effects of island subsidence and sea level rise (Moore and Fornari 1984). The reef's break-in-slope at –150 m is shown in Figs. 2 and 3. The reef creates a gently sloping shelf off the northwest portion of the study area that limits the amount of slumping along the coast. However, starting northwest of ‘Opihi Rock and continuing to the southeast, the offshore slope is extremely steep and the coast is characterized by a high (>6 m) sea cliff.

Subtle textural differences in the bathymetric data allow us to distinguish reef from lava flows. Figure 3 shows that the reef is covered by a lava flow, probably the 1400-year-old Pana‘ewa ‘a‘ā flow (Wolfe and Morris 1996a), north-northwest of approximately 19°38.6′N. Just southeast, but still north of Kaloli Point, the reef has been modified by several 0.5-km-wide slumps along the reef face. Due east of Kaloli Point, three additional narrow (a few hundred meters wide) slumps have modified the reef face. A second lava flow, much more subdued than the one to the northwest, covers 2.5 km of the reef southeast of 19°36.7′ N, 205°04.0′W. Based on its location, this flow is not ‘Ailā‘au but could be unit C or, more likely, some older flow not seen on land. The reef disappears near ‘Opihi Rock (Fig. 4). It has either been covered by younger Kīlauea flows or did not form to the east because of a higher rate of lava flow coverage that prevented its development. Immediately offshore from ‘Opihi Rock, a narrow lobe of lava drapes the steep slope for approximately 0.75 km to a depth of approximately 500 m (Fig. 4). This flow lobe is almost certainly a lobe of ‘Ailā‘au lava that entered the ocean over the cliff at ‘Opihi Rock.

Radiocarbon ages

'Ailā'au flows

We have determined radiocarbon ages on six new charcoal samples and report one previously unpublished radiocarbon date kindly supplied to us by F.A. Trusdell. The carbon samples collected during this study were carefully collected and cleaned to minimize contamination. In addition, only very small carbonized roots and twigs were selected for dating, because samples from larger trees or roots could yield erroneously old ages arising from the age of the tree at the time of lava inundation.

Evaluation of the reliability of the new and published dates requires knowledge of the analytical procedures employed. Charcoal samples ideally undergo a series of pretreatment steps to remove contamination by modern rootlets and adsorbed humates prior to analysis. Full pretreatment for samples prepared at the U.S. Geological Survey (W- or WW sample numbers marked by superscript "a" in Table 1; J. McGeehin, pers. commun.) consists of a 1-h 80 °C 1-N HCL wash to remove carbonate, a 2-h 80 °C 2% NaOH wash to remove absorbed humates, and a second 1-h 80 °C 1-N HCL wash to neutralize the alkali wash. Samples prepared for analysis at the University of Arizona receive a similar treatment, except that the NaOH wash is done overnight at room temperature and the second acid wash is also at room temperature (W. Beck and G.S. Burr, pers. commun.).

Only 7 of the 20 samples received full pretreatment, with one of these apparently a modern sample (W4573) rather than charcoal formed when the flows erupted. Three samples (W4449, W4661, and WW1525) received an abbreviated pretreatment consisting of an acid wash followed by a brief room-temperature NaOH wash. Such an abbreviated pretreatment is used if the submitted sample is too small to withstand the losses associated with full pretreatment. Several additional samples (W5110 and W5631) received only an acid wash. The remaining seven 'Ai la'au samples and sample W4177, from an older kipuka, were given no pretreatment. The small samples required for AMS dating (samples with either WW- or AA numbers) may offset the lack of pretreatment to some degree, because they can be handpicked to select only the cleanest, most vitreous charcoal. The lack of full pretreatment for so many of these samples almost certainly contributed to the large range of analytical ages, particularly the many ages younger than 350 radiocarbon years, determined for charcoal collected beneath the 'Ailā'au flows. Next, we evaluate the age population using several subsets of the age data.

Although the radiocarbon ages, evaluated uncritically, could be taken to indicate that the 'Ailā'au eruption lasted several centuries, we do not think that this is so. An inter-laboratory comparison of ^{14}C dates for replicate tree-ring samples has shown that uncertainties

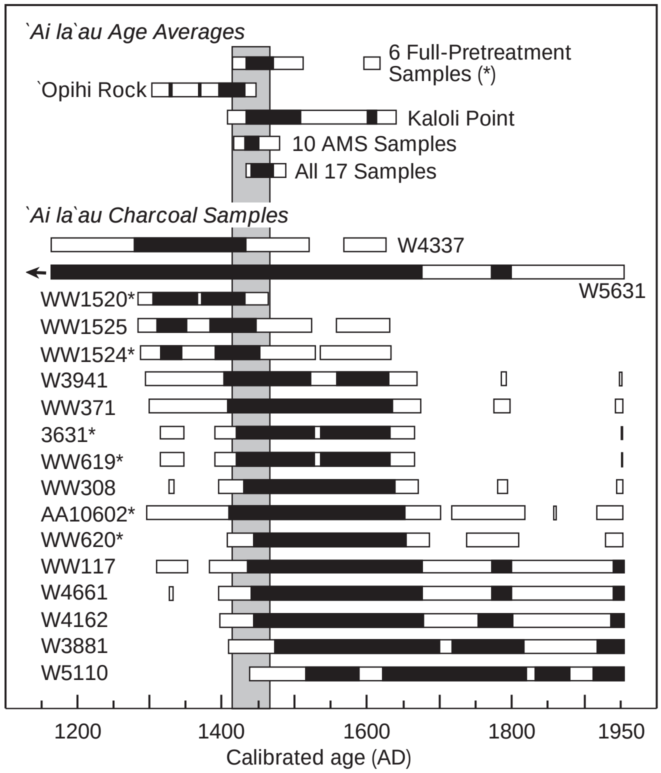

Fig. 5 Bar plot of each radiocarbon age calibrated using Stuiver and Reimer (1993) method A (intercept with curve). The *filled bars* represent 1-σ errors and the unfilled bars represent 2-σ errors. The reported analytical errors on each sample were doubled as explained in the text. The top five bars show averages of all 17 radiocarbon dates, the 10 AMS radiocarbon dates, the three new samples with ages between 420 and 430 radiocarbon years (Kaloli Point), the three new samples with radiocarbon ages between 520 and 530 radiocarbon years ('Opihi Rock), and the 6 samples that received full pretreatment (6 FPT). All the different groupings are consistent with an eruption age for the 'Ailā'au lava flows approximately AD 1445. The shaded band is 50 years wide and shows that all the sample ages and averages are consistent with eruption during a period of this duration

based on the counting statistics (one standard deviation) are generally too low and should be multiplied by a factor of between 2 and 3 (International Study Group 1982). Based on this study, we have calibrated the ages (using the radiocarbon calibration methods of Stuiver and Reimer 1993) after doubling their reported analytical errors (Fig. 5). All subsequent calendar ages refer to ages calibrated with this method. We have disregarded the three ages (<200, <200, 2160 radiocarbon years BP) superceded by subsequent samples from the same sites. Analysis of the 17 remaining dates shows that they are statistically identical (based on a chi-squared test) with an average age of 429 ± 28 radiocarbon years BP, equivalent to a calibrated age of AD 1449. At 2σ there is a 97% probability that the population formed between AD 1430 and 1510 and a 3% probability they formed between AD 1602 and 1615. The multiplicity of possible calendar age ranges (Fig. 5) reflects the nonuniform production of ^{14}C in the atmosphere through time. In addition, the non-linear relationship between radiocarbon ages and calendar ages can result in similar calendar ages from disparate radiocarbon ages, or vice versa.

We can group the dates to consider only those determined by accelerator mass-spectrometry (AMS). This group includes all the dates determined since 1987, except one (3631; Table 1), and eliminates the youngest four dates and the oldest two dates from the population. The remaining ten dates have an average age of 457±34 radiocarbon years BP, equivalent to a calibrated age of AD 1442. At 2 σ there is a 100% probability that the population formed between AD 1408 and 1489.

Another possible group of dates, using only those that received the full pretreatment described previously, reduces the population to only six samples. They have an average age of 443±43 radiocarbon years BP, equivalent to a calibrated age of AD 1445. At 2σ there is an 88% probability that the population formed between AD 1409 and 1519 and a 12% probablity that it formed between AD 1576 and 1625.

The results of our analysis using all 17 dates, the group of 10 AMS dates, or dates on only fully pretreated samples are very similar and indicate that the ʻAilāʻau flows most likely erupted approximately AD 1445±30. This age is 100 years older than that proposed by Holcomb et al. (1986). This analysis, however, provides no information on the possible duration of the eruption, despite the large range in reported radiocarbon ages. These pooled results are shown in Fig. 5.

There is apparent spatial control to our new ages. The three samples collected northwest of ʻAuwae Point (WW371, WW619, and 3631; Table 1; and Kaloli Point group in Fig. 5) have ages ranging from 420 to 430 radiocarbon years BP. They are statistically identical to one another and have an average age of 423±61 radiocarbon years BP, equivalent to a calibrated age of AD 1451. At 2σ there is a 64% probability that they formed between AD 1416 and 1530 and a 36% probability they formed between AD 1532 and 1635. This portion of the flow field includes lava transported in the Kazumura tube system (WW619 and probably WW371), one of the younger tubes in the flow field (Fig. 1). The other three new ages range from 520 to 570 years and were collected from the northeast portion of the flow field (WW1520, WW1524, and WW1525; Table 1; and the ʻOpihi Rock group in Fig. 5). They are also statistically identical to one another and yield an average age of 545±53 radiocarbon years BP. This age is equivalent to a calibrated age of AD 1409. At 2σ there is a 35% probability that they formed between AD 1305 and 1368 and a 65% probability that they formed between AD 1372 and 1446. The age ranges for these two groups overlap for the entire first half of the fifteenth century (Fig. 5). We conclude that, despite the apparent spatial distribution of these sample groups, they do not differ significantly in age. Both groups, and the entire ʻAilāʻau flow field, most likely erupted in the first half of the fifteenth century.

Kipukas

Published radiocarbon ages for lava flows underlying the ʻAilāʻau flows are rare. Rubin et al. (1987) report an age on an untreated sample of 3690±70 radiocarbon years BP or ~4030 calendar years BP (W4177, Table 1; 9B899, Table 3) for a unit B flow in a sugarcane field east of Keaʻau (Fig. 1). The sampled site was within the sugarcane field and was covered by thick ash (>1 m thick). However, the dated flow has the same paleomagnetic orientation as other nearby unit B flows. We suspect that this site has been perturbed by man and that the sampled site is a narrow lobe of unit B lava that flowed down a drainage within a much older flow beneath the sugarcane field. The thick ash may have been deposited on top of the flow during cane operations, because other nearby unit B flows are not covered by such thick ash.

We have added an age for unit A flows near ʻAuwae Point (B6735; Fig. 2; Table 3). The charcoal beneath this flow (AA18815; Table 1) has an age of 2604±54 radiocarbon years BP, equivalent to ~2750 calendar years BP.

Throughout the remainder of this paper we refer to all ages in calendar years, either AD or BP (from 1950), unless otherwise specified.

Chemistry of flows

Whole-rock chemical analyses are available from many locations in the ʻAilāʻau flow field (Wolfe and Morris 1996b), but they are difficult to use in discriminating different flows because of the effects of variable olivine contents of the flows and the large analytical uncertainties inherent in wet-chemical rapid-rock analyses. To minimize the likelihood of combining analyses from different flows, we used the paleomagnetic data to confirm that sampled flows identified as ʻAilāʻau actually belong to the flow field. The whole-rock analyses of the ʻAilāʻau samples range from aphyric (6.8 wt.% MgO) to picritic (23.4 wt.% MgO), with the majority of flows being sparsely olivine-phyric with whole-rock MgO contents of 7–9 wt.%. There is no systematic difference between the whole-rock data for the ʻAilāʻau flows and those from the older flows exposed in kipukas.

On the other hand, glass samples from the ʻAilāʻau flows (Table 2) have a much narrower range of MgO contents (6.0–7.0 wt.%) that are not randomly distributed within the flow field. Instead, the more MgO-rich glass samples were collected near the eruptive vent in Kīlauea Iki Crater, and the lower-MgO glass samples were collected at the coast approximately 40 km from the vent (Fig. 6). Concentrations of MgO for the ʻAilāʻau samples do not form a tight trend with distance

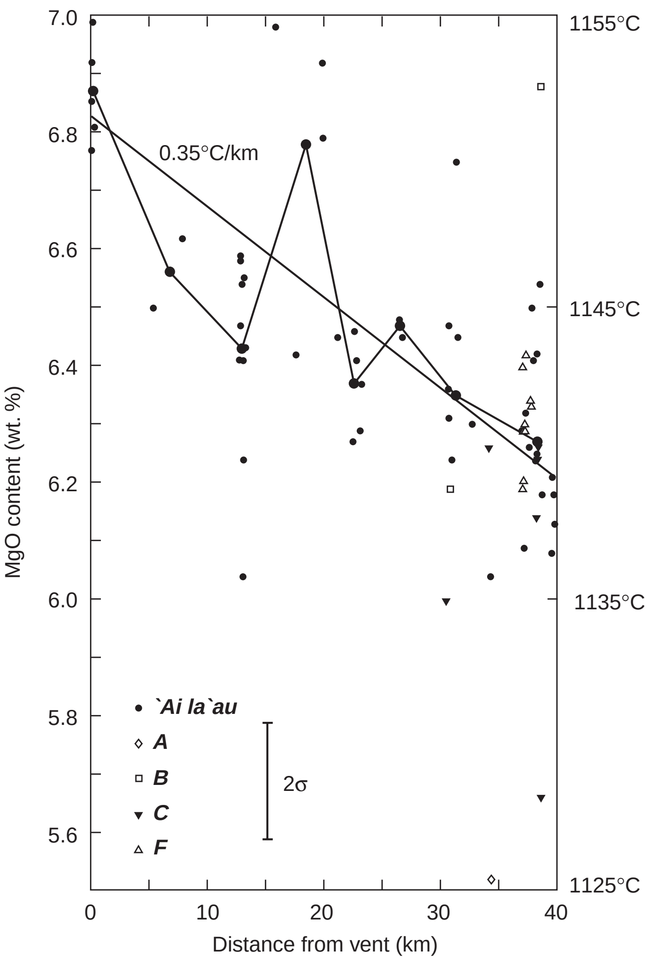

Fig. 6 Plot of MgO contents of collected glass rinds on surfaces of ‘Ailā‘au and other flow units vs distance from the center of Kīlauea Iki Crater (vent), roughly located at the center of the ‘Ailā‘au lava shield. The right-hand temperature scale is calculated from the MgO contents using Helz and Thornber (1987). *Small symbols* (see symbol key at lower left) are individual samples, and *larger solid* circles are averages for all ‘Ailā‘au samples within each 5-km increment. The ‘Ailā‘au lava crystallized olivine, augite, and plagioclase, and the glass chemistry evolved to lower MgO contents as the lava flowed inside tubes on its 40-km transit to the ocean. This evolution took place at an average rate of 0.025% MgO/km, equivalent to a cooling rate during transport of 0.35 °C/km (shown as a *straight line*). This cooling rate is approximately one fourth that measured during flow of Pu‘u ‘Ō‘ō lava down a much steeper slope on the southern flank of Kīlauea’s east rift zone (Cashman et al. 1994; C. Thornber, pers. commun.)

from the vent (Fig. 6). This scatter could indicate either that the melt temperatures varied somewhat during the eruption or that variations arose during the transport and emplacement of these flows. Quench temperatures, estimated using the Helz and Thornber (1987) geothermometer, range from 1135° to 1155 °C. The range of MgO contents at the coast is approximately 0.5 wt.%, which corresponds to an approximately 10 °C variation in quench temperatures. The glasses have quench temperatures ~14 °C cooler on average at the coast than near the vent, corresponding to a cooling rate of approximately 0.35 °C/km during transport through the tube system and during emplacement of the surface flows. The compositions, corrected for cooling during transport through tubes and during emplacement, suggest a narrow range of eruption temperature during this sustained eruption (from ca. 1152 to 1159 °C). These data also document the thermal efficiency of within-tube lava transport, even over distances as great as 40 km. The coherence of the glass data was unexpected, as we anticipated that variations in emplacement history and quenching would introduce large variations. This, however, is not what we observed.

For comparison, compositions of glass (collected as molten samples and quenched) from the current Pu‘u ‘Ō‘ō eruption are consistent with eruption temperatures ranging from 1147 to 1161 °C between 1986 and 1992 (Helz et al. 1991; Mangan et al. 1995). All but a few samples have calculated temperatures between 1152 and 1158 °C. Cooler quench temperatures near the coast have been attributed to cooling and crystallization during transport within the tube system (Cashman et al. 1994). For the current eruption, lava flows down the steep southern flank of Kīlauea’s east rift zone and the rate of cooling is estimated at approximately 1.4–1.8 °C/km (C. Thornber, pers. commun.). This cooling rate corresponds to a decrease in MgO content of the glass of 0.07–0.09 wt.% MgO/km. These rates are roughly four to five times those estimated for the ‘Ailā‘au flows. These data could be explained if the ‘Ailā‘au tubes were significantly better insulated by being larger, deeper, and with fewer skylights than the tubes in the Pu‘u ‘Ō‘ō flow field.

We also analyzed glass from flow units A, B, C, and F that, based on their chemical compositions, were all erupted from Kīlauea Volcano. Flows C and F have nearly identical major element compositions to the ‘Ailā‘au flows collected at similar distances from the summit. Flow units A and B have significantly different compositions, with unit A more differentiated (only 5.5 wt.% MgO) and unit B less differentiated (up to 6.9 wt.% MgO) than ‘Ailā‘au and units C and F. After correction for cooling during transport using the same rate used for the ‘Ailā‘au flows, unit B lava should have had an eruption temperature of approximately 1165 °C, slightly above the initial crystallization temperature for augite and plagioclase. Unit A lava, also corrected for temperature decrease during transport, should have had an eruption temperature of approximately 1145 °C. The inferred high viscosity of this low-temperature lava may have inhibited bubble loss and formation of a dense glassy rind.

Our general conclusions are that all sampled summit eruptions produced strongly fractionated lava flows erupted at temperatures between 1145 and 1165 °C, and that olivine, augite, and plagioclase crystallized from them as they were transported ~40 km to the coast in large, deep tube systems. Many of these flows, particularly the ‘Ailā‘au flows within 10–15 km of the coast, lost most of their gas bubbles during transport and were emplaced as dense, glass-topped flows similar to dense, glassy breakouts from tubes observed during both the Mauna Ulu (Peterson and Swanson 1974) and Puʻu ʻŌʻō eruptions (Mattox et al. 1993). The loss of such a large portion of the vesicles decreases the bulk viscosity of lava (Manga et al. 1998) and should facilitate transport through the long tube systems. Some parts of these flows, especially in the upper and middle parts of the ʻAilāʻau flow field, are strongly olivine phyric.

Paleomagnetic results

ʻAilāʻau flows

The site mean directions for all 37 sites in the ʻAilāʻau flows are listed in Table 3 and plotted in Fig. 7. For completeness, Table 3 includes data previously published by Holcomb (1981, 1987), Holcomb et al. (1986), and Hagstrum and Champion (1995), in addition to our 16 new sites. At sites with available dates (Fig. 7), the ages have been included and show no compelling trend in direction with age. These directions have a level of dispersion similar to that for other Hawaiian lava flows due to local magnetic anomalies and magnetic terrain effects (Hagstrum and Champion 1994). These directions have a Fisherian (circular) distribution, indicating that they were erupted quickly relative to paleosecular variation (PSV) of the geomagnetic field. The overall mean direction for the ʻAilāʻau lava flows is $I = 44.6°$, $D = 4.2°$, $\alpha_{95} = 0.8°$, $N = 37$.

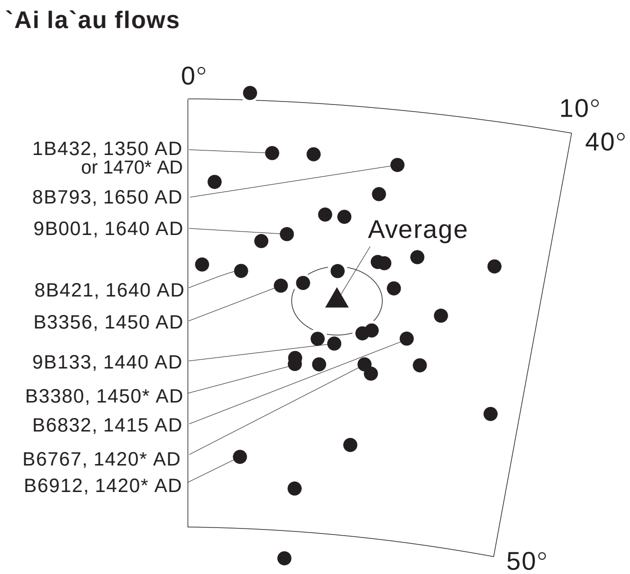

Fig. 7 Equal-area projection (lower hemisphere) of site-mean directions for the ʻAilāʻau lava flows (*dots*) listed in Table 3. Larger triangle with 95% confidence limits (*ellipse*) indicates the ʻAilāʻau site mean. Calibrated ^{14}C ages (Table 1; *asterisk* indicates sample with full pretreatment) are indicated with the corresponding (within 150 m) paleomagnetic site number (Table 3) to evaluate whether the dispersion in the ʻAilāʻau sites is caused by secular variation during the extended time the flow field was being emplaced. No relationship between age and site-mean directions is evident, suggesting either that the determined age sequence is not representative of the true time sequence, or that there was little, if any, secular variation during the emplacement of these flows

Kipukas

Site-mean directions for flows in kipukas surrounded by the ʻAilāʻau flows (Figs. 1, 2) are given in Table 3 and plotted in Fig. 8A. These directions form six groups that have been labeled A to F. Mean directions for these groups and the ʻAilāʻau flows have also been plotted in Fig. 8B; they have a wide range in inclination (13–45°) and relatively restricted range in declination (353° to 4°E). Ages have been assigned to these seven directional groups based on radiocarbon ages, geologic relations, and the reference PSV curve for Hawaiʻi (Hagstrum and Champion 1995).

An age of ~2750 BP for the group A flows (AA18815; Table 1) is generally consistent with the group's mean direction compared with the PSV reference curve (Fig. 8B), although the reference curve's inclinations are apparently too steep for this time and will be updated with these data. A group-B flow (9B899) has an age of 4030 BP (W4177), and the mean unit B direction corresponds well with directions of that age on the PSV reference curve. A single site near Hawaiian Beaches (B6864) has a direction similar to unit B but an unknown age. This flow, however, is an ʻaʻā flow erupted from the east rift zone, which separates it from the tube-fed pāhoehoe flows that make up unit B. Flows comprising unit C have a mean direction similar to that of the ʻAilāʻau flows but are stratigraphically below the 2750 BP unit A flows. Such steep inclinations occur prior to the oldest direction on the published PSV curve. We assign these flows an age of 5250 calendar years BP, because flows having similar steep inclinations occur on Hualalai and Mauna Kea Volcanoes (D. Champion, unpublished data) with equivalent radiocarbon ages between approximately 4500 and 4700 years. Site B6920, in an ʻaʻā flow probably erupted from the east rift zone, is along the coast just northwest of Hawaiian Beaches. It has the same paleomagnetic direction as tube-fed pāhoehoe unit D flows. However, because of its different flow morphology and distance from other unit D outcrops, we have not grouped it as a unit D flow. Although flow units D and E have directions that could correlate with those of younger ages on the reference PSV curve, stratigraphy and other geologic observations indicate that these flows are older and provide an upper age limit on the unit C flows.

Other age constraints

Altered ash on top of some flow units provides another age constraint on the timing of the summit overflows

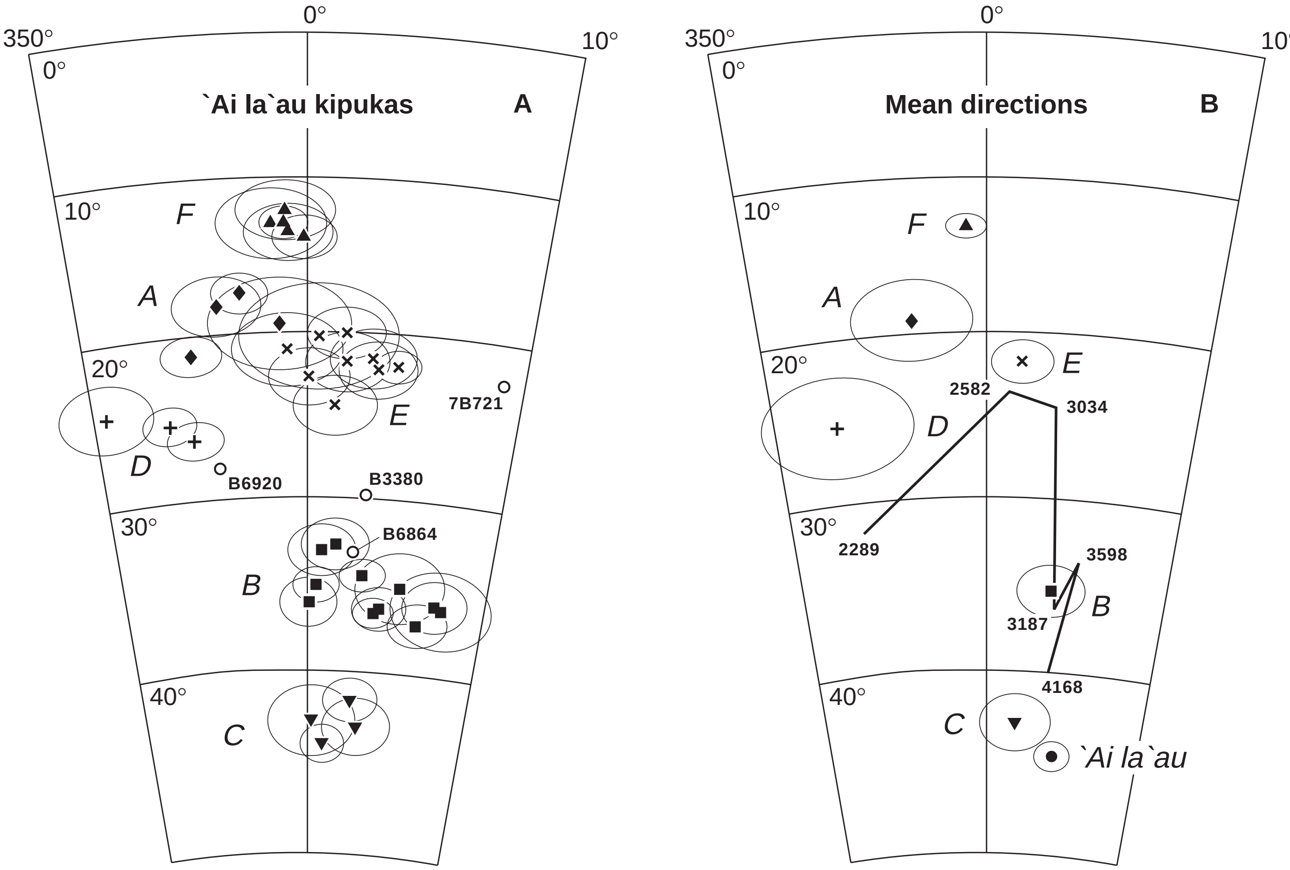

Fig. 8 **A** An equal-area projection of site-mean directions, with 95% confidence limits (α_{95}), for the kipukas listed in Table 3. The *open circles* with site labels and no confidence limits are mean directions for other Kīlauea or Mauna Loa flows. **B** An equal-area projection of mean directions with 95% confidence limits for each group of lava flows (see text). Also included is part of the PSV reference curve from 2200 to 4400 radiocarbon years BP (*solid line;* Hagstrum and Champion 1995). Values along the curve are averaged radiocarbon ages indicating averaged directions of data points within non-overlapping windows. All *symbols* indicate projection onto the lower hemisphere

examined in this study. The ‘Ailā‘au flows and 2750 BP unit A flows lack altered ash (soils) on their surfaces. The 4030 BP unit B flows, the estimated 5250 BP unit C flows, and the lower flow at paleomagnetic site B3380, are covered by thin altered ash (~2–3 cm), and flow units D, E, and F have thick altered ash (>10 cm). The altered ash on all of these flows was almost certainly erupted from Kīlauea Volcano and carried northeastward by counter-tradewinds. Two explosive eruptions are documented along the nearby lower east rift zone, at Pu‘ulena and Kapoho Cone, but both are less than 750 years old (Moore and Trusdell 1991) and therefore cannot be the source of any of the ash in the study area. Explosive eruptions occurred at, or near, the summit of Kīlauea in AD 1924, AD 1790 (Keanakāko‘i Ash), between 2060 and 2850 BP (Uwēkahuna Ash; Dzurisin et al. 1995), between approximately 3700 and 5590 BP (Easton 1987), between 5590 and 12,600 BP (Easton 1987), and between 23,000 and 28,000 radiocarbon years ago (Pāhala Ash; Easton 1987; Clague et al. 1995). Several older ash deposits (Mo‘o, Pōhaku, Halapē, and Kalele) are also present on Kīlauea (Easton 1987; Clague et al. 1995). Of these eruptions, the AD 1924, Keanakāko‘i, and Uwēkahuna ashes are too young, and their eruption products were not dispersed far enough from the summit (Dzurisin et al. 1995) to deposit measurable ash in the vicinity of the Hawaiian Paradise Park subdivision. On the other hand, the Pāhala Ash and older ash deposits appear to be significantly too old to be found on lava flows in the study area, with the exception of the sugarcane fields near Kea‘au.

The ash erupted between 3700 and 5590 BP is only 10–30 cm thick in the dated section at Nanaha Arroyo on Hilina Pali, 11 km south of Kīlauea Iki (Easton 1987). We think that this explosive eruption took place 3840 BP, the calibrated age of a charcoal sample (W4380) collected within the ash sequence at Wung Quarry near Volcano (Fig. 1; Rubin et al. 1987). If this correlation is correct, then the ash was deposited only a few hundred years after the unit B flows (4030 BP) were emplaced. This ash, by itself, also probably covers the unit C flows, giving them an upper age limit of ~5590 BP, consistent with our age assignment of 5250 BP based on a PSV correlation with other dated flows. This 3840 BP explosive eruption probably did not deposit as much ash as occurs on flow units D, E, and F.

The next older ash at Nanaha Arroyo may be a better match for the thicker ash on units D, E, and F because it is much thicker (ca. 1.5 m) and coarser at Nanaha Arroyo. Its thickness there indicates a bigger, more energetic eruption that was more likely to have dispersed abundant ash as far away as our study area in Puna. Since this ash erupted between approximately 5590 and 12,600 BP, we conclude that units D, E, and F are all older than 5590 BP.

The sea cliff along the northwestern part of the coastline provides an independent, though somewhat crude, method of constraining the ages of flows that crop out there. When lava flows enter the ocean, lava deltas slump seaward and create a cliff with an average height of approximately 6–8 m. This process has been observed repeatedly during the current Pu‘u ‘Ō‘ō eruption. Because the island is apparently subsiding more rapidly than coastal retreat occurs, the sea cliff height diminishes with time. We see this effect in our study area, with the ‘Ailā‘au flows having the highest sea cliffs (ca. 6 m), and progressively lower sea cliffs in the 2750 BP unit A flows (ca. 3.5 m), and the 5250 BP unit C flows (ca. 2.5 m). Extrapolating this trend of sea cliff height vs flow age suggests that units E and F, where the flow surface at the coast is now awash, are at least 9000 BP. Flow unit D is not found along the coast, but it occupies the area between flow units E and F. Unit D may have flowed down the contact between units E and F, in which case it would be the youngest of the three flows. Definitive evidence on which to base this interpretation, however, is presently lacking.

In summary, the stratigraphy for Kīlauea's northeast flank from youngest to oldest consists of the following units: The youngest unit is the ‘Ailā‘au flows, emplaced during a prolonged eruption centered on AD 1445 (505 BP). ‘Ailā‘au flows are on top of all other units. Unit A flows were emplaced at 2750 BP, and unit B flows were emplaced at ~4030 BP. Unit C flows underlie unit A flows and are inferred to have been emplaced at roughly 5250 BP, based on their stratigraphic position and paleomagnetic direction. Unit D has thicker ash cover and is probably older than unit C and younger than units E and F. Units E and F are most likely older than 9000 BP but probably younger than 18,000 BP (the age of the offshore reef that unit E and unit F flows do not cross). This stratigraphy is quite different from that depicted by Wolfe and Morris (1996a), in which our units A, B, C, D, and E were classified as 500–670 calendar years BP (400–750 radiocarbon years BP). Such old lava flows have previously been found only in the Hilina Basalt, exposed on Kīlauea's south flank.

In addition, there are several other flows identified by paleomagnetic data at single sites. Several of them are ‘a‘ā flows that probably originated along the east rift zone (B6864 and B6920; Table 3). The lower flow at paleomagnetic site B3380 (Table 3), however, is paleomagnetically distinct from unit B flows and could be from a younger flow field (~3100 radiocarbon years BP; Hagstrum and Champion 1995) of unknown but limited distribution. The soil on this flow is only a few centimeters thick, consistent with our interpretation that it is younger than unit C flows. The lava flow at paleomagnetic site 7B721 (Table 3) has a distinctive direction as well, and it may represent another old flow field of unknown, but limited, distribution. An unsampled flow, thought to be from Mauna Loa Volcano, underlies the sugarcane fields south of Kea‘au (light shaded area at W4177 in Fig. 1; Holcomb 1987; Wolfe and Morris 1996a). It is covered by >1 m of ash that indicates it is older than flow units A to E. We speculate that this flow is older than approximately 40,000 BP, because the youngest thick ash in the Hilo drill hole (10 km north of Kea‘au) is dated at >38,600 radiocarbon years (Beeson et al. 1996). This age is significantly older than the 5000 to 10,000 BP estimate of Wolfe and Morris (1996a).

Discussion

Volume of ‘Ailā‘au flows

Using the areal extent of the ‘Ailā‘au flow field on land and an approximation of the flows' average thickness, a straightforward, although imprecise, estimate of the flow field's volume can be made. The largest uncertainty in this calculation is the level of the original surface near the vent or, framed differently, the thickness of the flows that comprise the ‘Ailā‘au shield. We use 150 m for the thickness of flows at the shield, 5 m for the average thickness of flows in the lower quarter of the flow field, and ~430 km^2 for the total subaerial surface area, to estimate that the flow field contains approximately 6.5 ± 1 km^3 of lava. This estimate may be too high, as the average thickness of Pu‘u ‘Ō‘ō lava flows erupted during episode 48 average no more than 8–12 m (J. Kauahikaua, pers. commun.). A similar average thickness for the ‘Ailā‘au flows would yield a volume between 3.1 and 5.2 km^3. We prefer the greater average flow thickness and corresponding larger volume, because the ‘Ailā‘au flows were emplaced on more gentle slopes than were the episode 48 Pu‘u ‘Ō‘ō flows. Another correction that must be applied is to convert the lava volume to a dense-rock equivalent by removing the vesicles. We estimate that the dense ‘Ailā‘au lava flows contain approximately 20 vol.% gas bubbles, so we have reduced our volume estimate accordingly to 5.2 ± 0.8 km^3.

Previous volume estimates had to contend with an unknown quantity of ‘Ailā‘au lava that was interpreted to have entered the sea along a ~10-km stretch of coast. Our new mapping demonstrates that the only significant volume of ‘Ailā‘au flows to enter the ocean did so at Kaloli Point (Fig. 1). Moreover, the March 1998 bathymetric survey shows that the offshore reef's break-in-slope around Kaloli Point is well defined (Fig. 3), indicating that ‘Ailā‘au lava did not drape the reef. Offshore from Opihi Rock (Fig. 4), a small flow lobe drapes the slope down to a depth of approximately 500 m. This lobe is most probably ‘Ailā‘au but has a miniscule volume. Thus, we infer that the volume of ‘Ailā‘au lava to enter the ocean was essentially limited to that required to form Kaloli Point, and is approximately 0.07–0.09 km^3. This is well within the errors associated with the on-land volume estimates and does not significantly affect our total volume estimate.

Duration of the ‘Ailā‘au eruption

The extensive system of long lava tubes in the ‘Ailā‘au flow field (Fig. 1) is consistent with nearly continuous eruption. Tubes formed during the Mauna Ulu (Peterson and Swanson 1974; Peterson et al. 1994) and the Pu‘u ‘Ō‘ō eruptions (e.g., Kauahikaua et al. 1998) are maintained only during periods of continuous effusion. Even short eruptive hiatuses can lead to breakdown of the tubes, extrusion of surface flows, and, subsequently, formation of new tubes. Likewise, the large size of ‘Ailā‘au tubes, such as the Kazumura tube, indicate high effusion rates like those measured during the current eruption (Kauahikaua et al. 1996). The 5.2-km^3 estimated dense volume for the flow field could be erupted in approximately 50 years at the eruption rate sustained by the current Pu‘u ‘Ō‘ō eruption ($\sim$0.1 km^3/year; Denlinger 1997).

The radiocarbon and paleomagnetic data are consistent with this estimated eruption duration, although the paleomagnetic data cannot resolve such a short time due to the slow rate of paleosecular variation ($\sim$0.5° per century) during this time period (Hagstrum and Champion 1995). The paleomagenetic data simply indicate that the eruption could have any duration less than approximately 300 years. Likewise, the radiocarbon data, particularly the two groups of ages from the Kaloli Point and ‘Opihi Rock areas, suggest that the eruption had a duration of at least several decades, although this distinction is also at the statistical limit of the data.

Based on these considerations, we propose that the ‘Ailā‘au flows were emplaced during roughly 50 years of sustained activity, mainly in the first half of the fifteenth century. Some of the youngest flows were transported to the coast in the Kazumura tube and built Kaloli Point. The distinction between younger and older ‘Ailā‘au flows (specifically near Volcano Village) shown on recent maps by Wolfe and Morris (1996a) and Neal and Lockwood (in press) is not supported by either paleomagnetic or radiocarbon results presented in this study.

Geologic hazards

The northeast flank of Kīlauea has been covered by pāhoehoe flows erupted during sustained activity near the summit only three times in the past 5000 years. Of these flows, the ‘Ailā‘au flows covered the largest area. The other flow units either covered the northern portion (unit B) or narrow swaths through the central portion (units A and C) of the ‘Ailā‘au field. During this time, only the ‘Ailā‘au, unit A, and unit C flows reached the ocean, and only the ‘Ailā‘au flows entered the ocean over more than a few kilometers of coastline. The intervals between flows ranged from 1250 to 2200 years, with an average (based on only three quiescent intervals) of approximately 1600 years. Farther back in time, unit E flows in the southern part of the region and unit F flows in the northern part each covered significant areas, but neither covered as much ground as the ‘Ailā‘au flows. The lava flow hazards map (Mullineaux et al. 1987; Wright et al. 1992) places this area in hazard zone 3 because of the infrequent occurrence of lava flows. Our study confirms that the north flank has lower hazards than most of the remaining surface of Kīlauea Volcano.

Along the coast just northwest of the Hawaiian Beaches subdivision, several ‘a‘ā flows (B6920 and B6864; Table 3) that erupted along Kīlauea’s east rift zone have reached the ocean. These flows are farther northwest (by $\sim$1 km) than the current boundary between hazard zones 2 and 3. This small apparent increase of the hazard in this area is offset by the fact that the ‘Ailā‘au flows erupted approximately 100 years earlier than previously thought.

In addition to lava flow hazards, our mapping sheds light on other geologic hazards in the region. For example, the offshore geology appears related to the development of sea cliffs along the coast. Northwest of ‘Opihi Rock, which marks the southeastern end of the offshore –150 m reef, the offshore slope is gentle, and unit E flows are awash along the shoreline. Southeast of the reef’s end, the offshore slope is extremely steep, and a >6-m-high sea cliff has formed in the vicinity of ‘Opihi Rock, cutting back into the unit E flows. Where the steep slope offshore is adjacent to the coast, shoreline retreat raises cliff height, outstripping the combined effects of island subsidence and sea level rise. Where the reef buttresses the shoreline, the opposite is true. Coastal areas with high cliffs therefore indicate zones subject to rapid coastline retreat. Although high cliffs are prone to collapse, low cliffs along this stretch of coastline are susceptible to storm or tsunami transport of large boulders significant distances inland. We observed such strandline deposits and scattered boulders around several coastal homes in the Hawaiian Paradise Park subdivision near site B3356 (Fig. 2).

Implications for the evolution of Kīlauea Volcano

Our study of the ‘Ailā‘au flows demonstrates that sustained eruptions at Kīlauea, similar to the on-going Pu‘u ‘Ō‘ō eruption, can continue for perhaps 50 years. The two eruptions are not, however, identical, because the Pu‘u ‘Ō‘ō vents are in the middle east rift zone and the ʻAilāʻau vents were near Kīlauea's summit. It is unknown if the possible duration of an eruption is dependent on vent location.

The ʻAilāʻau flows are probably the youngest summit overflows from Kīlauea Volcano (Neal and Lockwood, in press), although Holcomb (1987) had earlier interpreted them to be slightly older than the Observatory flows on Kīlauea's west flank. The Observatory flows are not as well dated as the ʻAilāʻau flows. However, the eight available ages (Holcomb 1987; Wolfe and Morris 1996b; Neal and Lockwood, in press) have an average age of 500 ± 50 radiocarbon years BP, equivalent to a calibrated age of approximately AD 1430. This age is statistically the same as the AD 1445 age of the ʻAilāʻau flows reported here, although the two flows did not erupt simultaneously because they have distinct paleomagnetic directions (Holcomb 1987). We conclude that the available age data do not establish the sequence of these two summit shields and, unfortunately, their flows are not in contact with one another (Neal and Lockwood, in press). It is, however, critical to calibrate the radiocarbon ages to calendar years (because the calibration is notably non-linear in this time period; Stuiver et al. 1998), in order to evaluate the timing of the volcanic events that shaped the landscape at Kīlauea. What is clear is that Kīlauea's summit overflowed repeatedly during a relatively short period of time, starting with the younger Kāluʻe flows, also poorly dated at approximately 700 radiocarbon years BP (Neal and Lockwood, in press), equivalent to approximately AD 1290 calendar years. The south-directed younger Kāluʻe flows, Āhua flows, and Lua Manu flows; the northeast-directed Volcano flows; the southwest-directed Observatory flows show the distributions of these summit overflows (Neal and Lockwood, in press); and the east-directed ʻAilāʻau flows discussed here, all erupted in a time period as short as 150–200 calendar years. We suggest that this series of shields in and around the summit formed during what could be considered a single summit eruption that occupied several vents, in much the same way that the current Puʻu ʻŌʻō eruption has built several shields. If this is the case, then the roughly 50-year-long ʻAilāʻau eruption represents only a fraction of the duration of a longer-lasting eruption at Kīlauea's summit.

The age of the ʻAilāʻau eruption may help constrain the time when the modern caldera formed at Kīlauea's summit and when the earliest layers of the Keanakākoʻi Ash erupted (Swanson et al. 1998). It seems most likely that the summit caldera formed after the series of summit eruptions ended approximately AD 1470 (AD 1445 plus half the estimated duration of the ʻAilāʻau eruption); otherwise, these flows would have ponded within the newly formed caldera instead of spilling down the flanks of the volcano. Based on this argument, we suggest that the modern caldera postdates AD 1470. The Keanakākoʻi Ash Member of the Puna Basalt is stratigraphically on top of the Observatory and ʻAilāʻau flows. It is generally thought to have erupted in AD 1790, but Swanson et al. (1998) recently suggested that the Keanakākoʻi Ash erupted over a period of perhaps several hundred years. The age of the underlying ʻAilāʻau flows places a limit on the earliest possible beginning of the explosive eruptions that formed the Keanakākoʻi Ash.

Conclusion

Our geologic observations, mapping, and stratigraphy, paleomagnetic measurements, radiocarbon dating, and geochemical analysis of the ʻAilāʻau flows and their kipukas have shown that the north flank of Kīlauea Volcano has been covered, at least in part, by flows that overflowed the summit region as few as three times in the past 5000 years, and as few as seven times in the last 10,000 years. The youngest of these summit overflows, the ʻAilāʻau flows, were emplaced during an approximately 50-year period probably in the first half of the fifteenth century. Although there may be more undetected flows, such eruptive events appear to be relatively infrequent, with one occurring on average approximately every 1600 years. The shortest interval between events is approximately 1250 years (between units A and B and units B and C), and the longest known interval is 2200 years (unit A and ʻAilāʻau). Each of these sustained summit, or near summit, eruptions produced tube-fed pāhoehoe flows that neared or reached the sea. The ʻAilāʻau flows entered the Pacific Ocean mostly near Kaloli Point between paleomagnetic sites B3356 and B3458 (Fig. 2). ʻĀʻa flows erupted along the east rift zone extend northwestward from near Cape Kumukahi to paleomagnetic site B6864. Chemical analyses of quenched glass of group F flows northwest of Kaloli Point show that they also were erupted from Kīlauea and not from Mauna Loa.

Of the flows from near-summit sustained eruptions found in kipukas, none appear to have as large an areal extent as the overlying ʻAilāʻau flows. Unit F occurs along the coast only northwest of Kaloli Point (Fig. 2), and units A, C, and E are found only southeast of Kaloli Point. Units A, B, and D crop out over a greater area away from the coast but are far less extensive than the ʻAilāʻau flows. Clearly the outlines of the underlying flows have been obscured by overlying flows, but exposures of the older flows at the coast away from Kaloli Point are excellent, and we sampled all of the different units in these regions.

The uniformly steep paleomagnetic directions for the ʻAilāʻau flows (Fig. 7), observed at sampling localities from Kīlauea's summit to the coast, indicate that the reference PSV curve (Hagstrum and Champion 1995) needs modification to reflect a steeper field direction at Hawaiʻi approximately 505 calendar years BP.

Acknowledgements The fieldwork for this study was completed while DAC was at the Hawaiian Volcano Observatory and was supported by the U.S. Geological Survey. The David and Lucille Packard Foundation generously provided the funding to complete this study and to conduct the offshore survey. Hawaiian Volcano Observatory volunteers L. Forman, N. Kanjorski, B. Kuhns, and C. Tozer assisted in the field and with sample preparation. F. Trusdell assisted with drilling and orientation of cores at several of the paleomagnetic sites and kindly permitted us to include a ^{14}C age of charcoal he collected from site WW620. J. Kauahikaua provided a GIS compilation of the locations of the lava tubes in the region. We thank R. Holcomb, J. Kauahikaua, J. Reynolds, F. Trusdell, and E. Wolfe for reviews of the manuscript that helped us clarify both our thinking and the presentation of our ideas.

References

Allred K, Allred C (1997) Development and morphology of Kazumura Cave, Hawai‘i. J Cave Karst Stud 59:67–80

Beeson MH, Clague DA, Lockwood JP (1996) Origin and depositional environment of clastic deposits in the Hilo drill hole, Hawai‘i. J Geophys Res 101:617–629

Buchanan-Banks JM (1993) Geologic map of the Hilo 7 1/2’ quadrangle, island of Hawai‘i. US Geol Surv Misc Investigations Series Map I-2274

Cashman KV, Mangan MT, Newman S (1994) Surface degassing and modifications to vesicle size distributions in active basalt flows. J Volcanol Geotherm Res 61:45–68

Christiansen RL (1979) Explosive eruption of Kīlauea Volcano in 1790. In: Decker RW, Drake C, Eaton G, Helsley C (eds) Hawai‘i Symposium on Intraplate Volcanism and Submarine Volcanism, Hilo, Hawai‘i, 16–22 July 1979. US Geol Survey, Hilo, Hawai‘i, p 158

Clague DA, Beeson MH, Denlinger RP, Mastin L (1995) Ancient ash deposits and calderas at Kīlauea Volcano. EOS Trans Am Geophys Union 76:F666

Denlinger RL (1997) A dynamic balance between magma supply and eruption rate at Kīlauea Volcano, Hawai‘i. J Geophys Res 102:91–100

Dzurisin D, Lockwood JP, Casadevall TJ, Rubin M (1995) The Uwēkahuna Ash Member of the Puna Basalt: product of violent phreatomagmatic eruptions at Kīlauea Volcano, Hawai‘i, between 2800 and 2100 ^{14}C years ago. J Volcanol Geotherm Res 66:163–184

Easton RM (1987) Stratigraphy of Kīlauea Volcano. US Geol Surv Prof Pap 1350:243–260

Fisher RA (1953) Dispersion on a sphere. Proc R Soc Lond A217:295–305

Hagstrum JT, Champion DE (1994) Paleomagnetic correlation of Late Quaternary lava flows in the lower east rift zone of Kīlauea Volcano, Hawai‘i. J Geophys Res 99:679–690

Hagstrum JT, Champion DE (1995) Late Quaternary geomagnetic secular variation from historical and ^{0} ^{14}C-dated lava flow on Hawai‘i. J Geophys Res 100:393–403

Helz RT, Thornber CR (1987) Geothermometry of Kīlauea Iki lava lake, Hawai‘i. Bull Volcanol 49:651–668

Helz RT, Heliker C, Mangan M, Hon K, Neal CA, Simmons L (1991) Thermal history of the current Kīlauean east rift eruption. EOS Trans Am Geophys Union 72:557–558

Holcomb RT (1981) Kīlauea Volcano, Hawai‘i: chronology and morphology of the surficial lava flows. US Geol Surv Open-File Rep 81-354:1–321

Holcomb RT (1987) Eruptive history and long-term behavior of Kīlauea Volcano. US Geol Surv Prof Pap 1350:261–350

Holcomb RT, Champion D, McWilliams M (1986) Dating recent Hawaiian lava flows using paleomagnetic secular variation. Geol Soc Am Bull 97:820–839

International Study Group (1982) An inter-laboratory comparison of radiocarbon measurements in tree rings. Nature 298:619–623

Kauahikaua JP, Mangan M, Heliker CC, Mattox T (1996) A quantitative look at the demise of a basaltic vent: the death of Kupaianaha, Kīlauea Volcano, Hawai‘i. Bull Volcanol 57:641–648

Kauahikaua J, Cashman KV, Mattox TN, Heliker CC, Hon KA, Mangan MT, Thornber CR (1998) Observations on basaltic lava streams in tubes from Kīlauea Volcano, island of Hawai‘i. J Geophys Res 103:303–323

Kirch PV (1985) Feathered gods and fishhooks: an introduction to Hawaiian archaeology and prehistory. University of Hawai‘i Press, Honolulu

Ludwig KR, Szabo BJ, Moore JG, Simmons KR (1991) Crustal subsidence rate off Hawai‘i, determined from $^{234}U/^{238}U$ ages of drowned coral reefs. Geology 19:171–174

Manga M, Castro J, Cashman KV, Loewenberg M (1998) Rheology of bubble-bearing magmas. J Volcanol Geotherm Res. 87:15–28

Mangan MT, Heliker CC, Mattox TN, Kauahikaua JP, Helz RT (1995) Episode 49 of the Pu‘u ‘O‘O-Kupaianaha eruption of Kīlauea Volcano: breakdown of a steady-state eruptive era. Bull Volcanol 55:407–413

Mattox TN, Mangan MT (1997) Littoral hydrovolcanic explosions: a case study of lava–seawater interaction at Kīlauea Volcano. J Volcanol Geotherm Res 75:1–17

Mattox TN, Heliker CC, Kauahikaua JP, Hon K (1993) Development of the 1990 Kalapana flow field of Kīlauea Volcano, Hawaii. Bull Volcanol 55:407–413

McPhie J, Walker GPL, Christiansen RL (1990) Phreatomagmatic and phreatic fall and surge deposits from explosions at Kīlauea volcano, Hawaii, 1790 A.D.: Keanakakoi Ash Member. Bull Volcanol 52:334–354

Moore JG, Fornari DJ (1984) Drowned reefs as indicators of the rate of subsidence of the island of Hawai‘i. J Geol 92:752–759

Moore RB, Trusdell FA (1991) Geologic map of the lower east rift zone of Kīlauea Volcano, Hawai‘i. US Geol Surv Misc Invest Ser Map I-2225

Mullineaux DR, Peterson DW, Crandell DR (1987) Volcanic hazards in the Hawaiian Islands. US Geol Surv Prof Pap 1350:599–624

Neal CT, Lockwood JP (in press) Geologic map of the summit region of Kīlauea Volcano, Hawai‘i. US Geol Surv I-Map

Peterson DW, Swanson DA (1974) Observed formation of lava tubes during 1970–71 at Kīlauea Volcano, Hawai‘i. Stud Speleol 2:209–222

Peterson DW, Holcomb RT, Tilling RI, Christiansen RL (1994) Development of lava tubes in the light of observations at Mauna Ulu, Kīlauea Volcano, Hawai‘i. Bull Volcanol 56:343–360

Rubin ME, Gargulinski LK, McGeehin JP (1987) Hawaiian radiocarbon dates. US Geol Surv Prof Pap 1350:213–242

Stuiver M, Reimer PJ (1993) Extended ^{14}C data base and revised CALIB 3.0 ^{14}C age calibration program. Radiocarbon 35:215–230

Stuiver M, Reimer PJ, Bard E, Beck JW, Burr GS, Hughen KA, Kromer B, McCormac FG, v. d. Plicht J, Spurk M (1998) INTCAL98 Radiocarbon age calibration 24,000–0 cal B.P. Radiocarbon 40:1041–1083

Swanson DA (1973) Pāhoehoe flows from the 1969–1971 Mauna Ulu eruption, Kīlauea Volcano, Hawai‘i. Geol Soc Am Bull 84:615–626

Swanson DA, Fiske RS, Rose TR, Kenedi CL (1998) Prolonged deposition of the Keanakāko‘i Ash Member, Kīlauea. EOS Trans Am Geophys Union 79:F937

Westervelt WD (1916) Hawaiian legends of Volcanoes. Honolulu, Charles E Tuttle, reprinted 1963 (Tokyo)

Wolfe EW, Morris J (1996a) Geologic map of the Island of Hawai‘i. U.S. Geol Surv Misc Invest Ser Map I-2524-A

Wolfe EW, Morris J (1996b) Sample data for the geologic map of the Island of Hawai‘i. US Geol Surv Misc Invest Ser Map I-2524-B

Wright TL, Chu JY, Esposo J, Heliker C, Hodge J, Lockwood JP, Vogt SM (1992) Map showing lava-flow hazard zones, Island of Hawai‘i, scale 1:250,000. US Geol Surv Misc Field Studies Map MF-2193